Global Change Biology

WILEY

Global Change Biology

RESEARCH ARTICLE OPEN ACCESS

Sex-Linked Differentiation in Commercially Exploited Fishes: Rethinking Population Structure in Dynamic Marine Environments

Courtney E. C. Gardiner[1] | Sophie von der Heyden[1,2] | Conrad A. Matthee[1] | Einar E. Nielsen[3] | José M. Pujolar[4] | Rita Castilho[5,6,7] | Regina L. Cunha[5,6] | Joana I. Robalo[8] | Deon Durholtz[9] | Tracey P. Fairweather[9] | Johannes N. Kathena[10] | Romina Henriques[2,11]

[1]Evolutionary Genomics Group, Department of Botany and Zoology, Stellenbosch University, Stellenbosch, South Africa | [2]School for Climate Studies, Stellenbosch University, Stellenbosch, South Africa | [3]National Institute of Aquatic Resources, Technical University of Denmark, Silkeborg, Denmark | [4]Centre for Gelatinous Plankton Ecology and Evolution, Technical University of Denmark, Kongens Lyngby, Denmark | [5]University of Algarve, Faro, Portugal | [6]Centre of Marine Sciences (CCMAR), Faro, Portugal | [7]Pattern Institute, Faro, Portugal | [8]Marine and Environmental Sciences Centre (MARE), Aquatic Research Network (ARNET), Instituto Universitário de Ciências Psicológicas (ISPA), Lisbon, Portugal | [9]Department of Forestry, Fisheries, and the Environment (DFFE), Cape Town, South Africa | [10]Ministry of Fisheries and Marine Resources (MFMR), Swakopmund, Namibia | [11]Department of Biochemistry, Genetics, and Microbiology, University of Pretoria, Pretoria, South Africa

Correspondence: Romina Henriques (romina.henriques@up.ac.za)

Received: 10 June 2025 | **Revised:** 24 August 2025 | **Accepted:** 10 September 2025

Funding: This work was supported by Fundação para a Ciência e Tecnologia (MARE/UIDB/MAR/04292, MARE/UIDP/04292, LA/P/0069/20), Fundação para a Ciência e a Tecnologia (UIDB/04326/2020, UIDP/04326/2020, LA/P/0101/2020), 2019-2020 BiodivERsA joint call for research proposals, under the BiodivClim ERA-Net COFUND programme, and with the funding organisations and Innovation Fund Denmark (0156-00018B).

Keywords: fisheries management | local adaptation | marine genomics | *Merluccius paradoxus* | population genomics | southeastern Atlantic | whole-genome sequencing

ABSTRACT

Understanding how genomic structure links with ecological and evolutionary processes is critical for forecasting species responses to dynamic marine environments, especially in commercially exploited marine species, where fishing pressure can impact genomic integrity. Here we investigate *Merluccius paradoxus*, a commercially exploited demersal fish that appears to be undergoing a range expansion along the southern African coastline. Using whole-genome sequence data of individuals from across the species' distribution ($n = 37$), we reveal that sex-linked divergence, rather than geography, is the principal driver of genomic variation, challenging conventional assumptions of regional geographic population structure. Divergence was concentrated on autosomal regions (primarily large regions on Chromosomes 1 and 2), rather than known sex-determining (SD) regions (Chromosome 9), and did not have structural variants or extended linkage disequilibrium (LD). Instead, patterns were consistent with sex-specific directional selection acting on genes enriched for neuronal function, metabolism and muscle development, traits that are likely linked to behaviour, physiology and environmental tolerance. Males had reduced nucleotide diversity (π), low observed heterozygosity (H_o) and longer runs of homozygosity (ROH) in these regions, suggesting recent selective sweeps or a reduced effective population size (N_e). Together with spatial differences in sex distribution and genomic diversity metrics, results suggest that males and females may differ in both range dynamics and adaptive potential. As *M. paradoxus* continues to shift its distribution across geo-political boundaries, sex-biased adaptation may have important consequences for reproductive output, resilience and sustainable fisheries management under a changing climate. This study highlights the need to incorporate sex-linked genomic variation into conservation planning, particularly in transboundary systems vulnerable to cumulative pressures of fishing and environmental change.

1 | Introduction

Global fisheries are a crucial source of nutrition, income and livelihoods, with the projected increase in demand for aquatic protein underscoring the urgent need for sustainable fishing practices (Belton and Thilsted 2014). Many exploited fish species face pressure from both overfishing and ongoing climate change (Sumaila et al. 2023; Zhao et al. 2022), where populations with a history of intense exploitation are particularly vulnerable to environmental extremes due to reduced population sizes and, possibly, lower genomic diversity (Pinsky and Byler 2015; Pinsky and Palumbi 2014). High fishing pressure can alter population structure (Gandra et al. 2021), reduce genomic diversity (Pinsky and Palumbi 2014) and decrease effective population sizes (Kuparinen et al. 2016), reducing adaptive potential and threatening the long-term persistence of these species (Pinsky and Palumbi 2014). The interaction between fishing and climate is compounding (Waples and Audzijonyte 2016), with combined effects already documented in species such as Atlantic cod (*Gadus morhua*; Engelhard et al. 2014) and Atlantic herring (*Clupea harengus*; Beaudry-Sylvestre et al. 2022; Slotte et al. 2025).

In marine systems, range expansions can occur as species recover from historical exploitation or respond to changing environmental conditions (Baudron et al. 2020; Hastings et al. 2020; Pinsky et al. 2020). The ecological and genomic consequences of these expansions, particularly those driven by environmental change, have been widely documented (e.g., Bors et al. 2019; Jacobs et al. 2019; Mendoza-Portillo et al. 2023). These expansions often follow a 'leading-edge' pattern, with populations expanding into new or historically occupied habitats (Baudron et al. 2020; Engelhard et al. 2014; Pinsky et al. 2020). While temperature is a key driver influencing distribution, other environmental factors such as oxygen availability, ocean acidification, upwelling patterns, productivity and salinity also influence habitat suitability for marine species (García Molinos et al. 2022). Range-edge populations often exhibit distinct genomic signatures shaped by both neutral and adaptive processes (Fifer et al. 2022; Ramos et al. 2018), where founder effects can lead to reduced diversity and shifts in allele frequency due to gene surfing, where certain alleles rise in frequency at the leading edge (Fifer et al. 2022; Wang et al. 2022), although multiple expansion waves can counteract these effects (Nielsen et al. 2024). Concurrently, local adaptations may occur in response to novel environmental pressures at the range edge. For instance, range-edge populations in the damselfly (*Ischnura elegans*) have adapted to climate-related variables including temperature, wind speed and precipitation (Dudaniec et al. 2018).

Although many marine fishes show weak overall genomic differentiation throughout their range due to historically large effective population sizes, high dispersal potential and high fecundity (Hirao et al. 2024; Jose et al. 2023), local adaptation can lead to cryptic differentiation even under high gene flow (Jiménez-Mena et al. 2019; Pujolar et al. 2025). Further, marine fishes exhibit diverse SD systems, shaped by environmental variability and rapid evolutionary turnover (Martínez et al. 2014). Sex-biased dispersal, spatially skewed sex ratios and sexual dimorphism in behaviour, physiology, or life history traits additionally shape genomic structure (Estévez-Barcia et al. 2025). Sex-specific dynamics can generate differentiation independent of geography, particularly if selection acts on sex-linked or sexually antagonistic traits (Barson et al. 2015; Eyer et al. 2019). In species with sexual size dimorphism, fishing gear that targets larger individuals may disproportionately remove one sex, typically females, thereby skewing sex ratios (Eklund and Targett 1990; von der Heyden et al. 2014). If sex ratios are already spatially variable, uneven fishing pressure may compound these differences. As such, understanding the joint influence of fishing, environmental change and sex-specific biology is critical for predicting species resilience in a changing ocean.

The Atlantic–Indian Ocean transition zone around southern Africa represents a valuable system for investigating dynamics around shifting distributions and population expansions of commercially exploited species, due to its steep environmental gradients and long history of commercial exploitation of demersal and pelagic stocks (Hutchings et al. 2009; Teske et al. 2011). The southern African marine environment is highly heterogeneous, shaped by stark environmental gradients and frequent disruptions to gene flow of regional species (Lett et al. 2024). Intense, perennial upwelling and high productivity dominate the west coast (Lamont et al. 2018), while the east coast experiences warmer, more stable waters with weaker seasonal upwelling (Hancke et al. 2023), contributing to regionally variable selective pressures. These regional environmental features influence the distribution and structure of many coastal and offshore commercially exploited marine species (Dalongeville et al. 2022), including leervis (*Lichia amia*; Henriques et al. 2012), Pacific sardine (*Sardinops sagax*, Teske et al. 2021), Cape hakes (*Merluccius capensis* and *Merluccius paradoxus*; Forde et al. 2025; Henriques et al. 2016) and kingklip (*Genypterus capensis*; Schulze et al. 2020). Despite the significant economic importance of marine resources that straddle a number of geopolitical boundaries, research on commercially valuable marine species in this marine climate change hotspot (Hobday and Pecl 2014) remains limited.

The deep-water hake (*M. paradoxus*) is a commercially important demersal species distributed from southern Angola to the east coast of South Africa, possibly extending into southern Mozambique (DFFE 2023). Although historic distribution prior to the 1980s is not well documented, available data since then suggest that the species has maintained a broad distribution across the Benguela and Agulhas Current systems (DFFE 2023). The species overlaps in distribution with the shallow-water hake (*M. capensis*), and while both species are assessed and managed as a single stock in Namibia, they are assessed separately (using gender-disaggregated assessment models) but managed jointly in South Africa. Historically, both hake species experienced appreciable stock declines during a period of overexploitation and poor recruitment in the 1960s–70s (DFFE 2023). With the subsequent implementation of effective management strategies, the status of hake stocks in South Africa and Namibia has improved, with spawning biomass of both hake species now above minimum sustainable yield (MSY) in South Africa (DFFE 2023). In Namibia, stocks remain below MSY (Marine Stewardship Council 2023), but the fishery has recently been certified by the Marine Stewardship Council (MSC; MSC 2020), with conditions having been set in place to promote recovery and improve sustainability.

The core range of *M. paradoxus* spans the West and South Coasts of South Africa, although the primary spawning ground lies

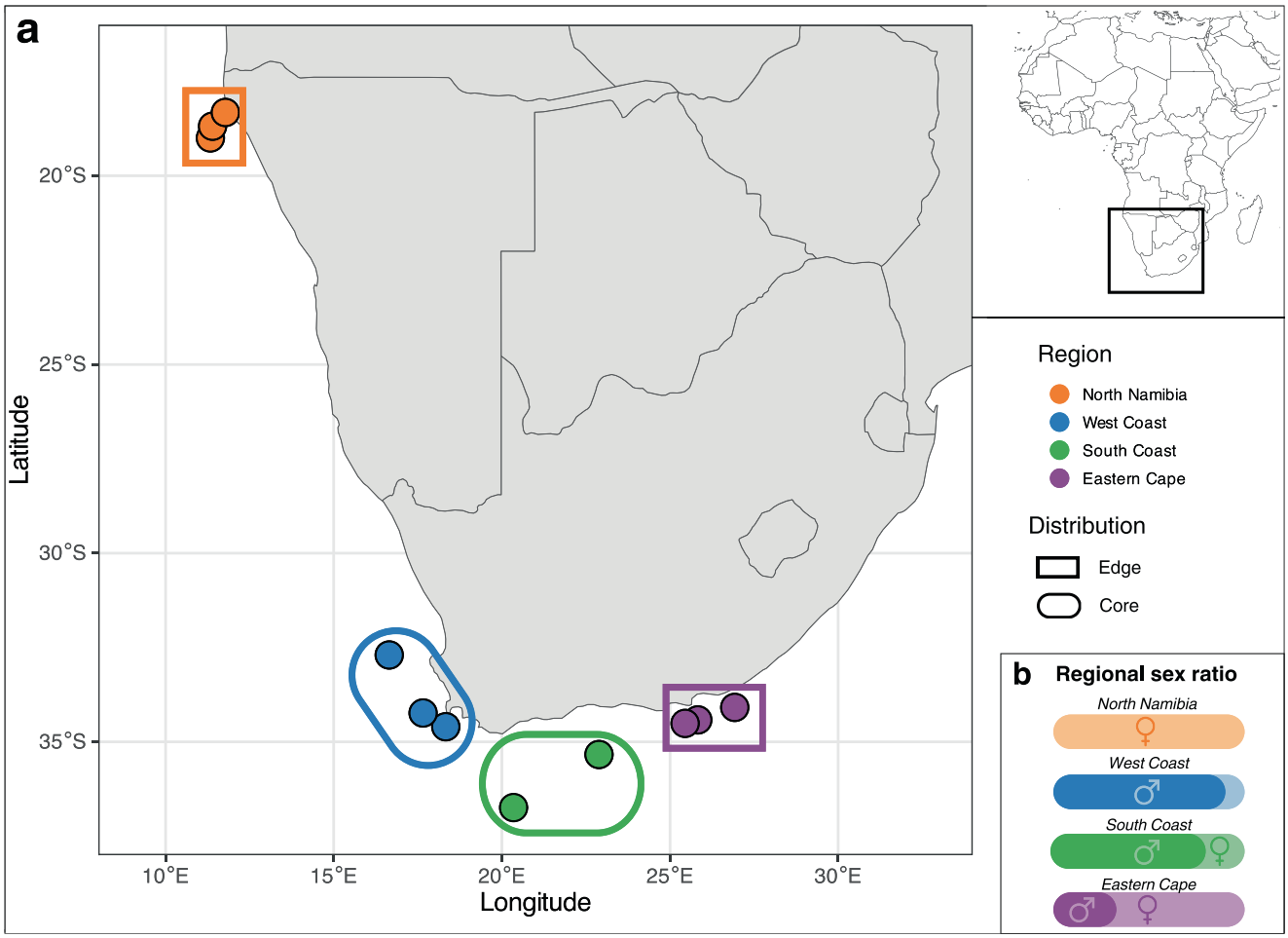

FIGURE 1 | (a) Sites locations for *Merluccius paradoxus*, with sites colour-coded by region. Shapes indicate classification as core (oval) or edge (rectangle) regions of the species' distribution. The inset shows the study area in relation to the African continent. (b) Proportion of male (♂) and female (♀) individuals in the samples collected from each site. Light shades represent females (♀), while darker shades represent males (♂). Map lines delineate study areas and do not necessarily depict accepted national boundaries.

between Elands Bay and the western Agulhas Bank (31°–34° S; Strømme et al. 2016). A smaller spawning ground has also been recorded off the eastern Agulhas Bank, off the southeast coast (26°–27° E; Jansen et al. 2015). In Namibia, spawning individuals are rare, and no consistent spawning activity has been documented (Jansen et al. 2015). Recent increases in the abundance of various size classes in Namibian waters (Strømme et al. 2016), as well as expansion eastwards towards Durban off the East Coast of South Africa (Fennessy, S., pers. comm), suggest a potential range expansion into previously underoccupied habitats. While these trends may reflect a response to environmental change, they more plausibly indicate population recovery following historical overexploitation. Importantly, the species' distribution core appears stable, with observed expansions occurring at both the northern and eastern edges of its range. This bi-directional expansion contrasts with the leading–trailing edge pattern typical of climate-driven range shifts (Pinsky et al. 2020; e.g., *G. morhua*; Engelhard et al. 2014), where core habitats shift in response to changing conditions.

Across its range, *M. paradoxus* shows pronounced spatial variation in sex ratios: adult females are more abundant in Namibian waters (Kathena, J., pers. comm.; often exceeding 75%; Figure 1), while males are slightly more prevalent off the West Coast of South Africa, where the proportion of males in the overall West Coast survey abundance estimates typically ranges from 55% to 60% (although the proportion of any given sex can frequently exceed 75% of the *M. paradoxus* catch at individual stations; Figure 1; Figure S1). To date, only one study has reported skewed sex ratios in a specific region, Table Bay, in South Africa (Botha 1986). While the specific mechanism of sex determination in *M. paradoxus* remains unknown, such skewed sex ratios in a system with heterogeneous environmental gradients and fishing pressure may reflect sex-specific selection, behaviour, or dispersal. In particular, the observed geographic pattern in sex ratios raises the possibility of environmentally driven sex determination. While *M. paradoxus* exhibits sexual size dimorphism, with males growing slower than females (Wilhelm et al. 2015), no consistent differences in behaviour or dispersal between the sexes have been recorded. In other hake species, however, sexual dimorphism has been recorded in the drumming muscles and lipid levels in *M. merluccius* (Groison et al. 2011; Panfili et al. 2024), and white muscle fibre composition in *Merluccius hubbsi* (Calvo 1989), making it therefore possible that similar development differences occur in *M. paradoxus*. However, to date, there is no conclusive evidence on the

mechanism responsible for the observed geographically skewed sex ratios in *M. paradoxus*.

Given their long-standing exploitation, as well as the transboundary distribution of *M. paradoxus*, range expansion and sex-biased distribution could exacerbate management challenges, as well as mismatches between current fishing practices, policies and future stock distributions. Further, both contemporary and historic levels of genetic diversity are relatively low compared to other commercially exploited demersal marine species such as the Atlantic cod (*Gadhus morhua*; Pinsky et al. 2021), or even the European hake and Shallow-water hake (*M. merluccius* and *M. capensis*; Henriques et al. 2016), suggesting a bottleneck or founder event potentially indicating historic population collapse (Henriques et al. 2016; von der Heyden et al. 2007a). This likely reflects the intense overexploitation experienced by the species in the 1960–70's.

In this study, we used whole-genome sequencing (WGS) data from individuals sampled across the species' range to assess how genomic variation in *M. paradoxus* is structured across environmental and biological factors, including the distribution of male and female fish. Specifically, we aimed to (1) assess genomic diversity and inbreeding patterns across the species' range and throughout the genome, (2) evaluate genome-wide fine-scale patterns of genomic differentiation and identify genomic regions under putative selection, (3) investigate how factors including sex, geographic distribution and depth contribute to observed genomic structure and (4) explore underlying mechanisms of differentiation through linkage disequilibrium (LD) analyses and gene enrichment of divergent regions.

While we expected to detect cryptic population structure at the range edges, potentially linked to environmental gradients or isolation by distance, we instead detected strong sex-linked genomic differentiation. This result was surprising given the few known spawning grounds for *M. paradoxus* and suggests that biological rather than geographic processes may be the principal drivers of population structure in this species. Our findings are particularly relevant given increases in hake abundance in Namibia and along the South African East Coast, which may reflect a range expansion following historical overexploitation and subsequent recovery. Together, our results challenge assumptions around geographical structuring in marine population genomics and underscore the importance of considering sex-specific processes in the management of exploited marine species, and in the study of distributional shifts.

2 | Materials and Methods

2.1 | Study Area and Sampling

Forty *M. paradoxus* samples were collected for medium coverage (20×) Whole Genome Sequencing (WGS) across the species' range, covering the western (Northern Namibia), eastern (Eastern Cape, South Africa) and core (West and South Coasts of South Africa) regions (Figure 1; see Table S1). Dorsal muscle tissue samples were preserved in 95% ethanol and stored at 4°C. Samples were collected during South African (Department of Fisheries, Forest and Environment, South Africa and CapMarine, South Africa) and Namibian (Ministry of Fisheries and Marine Resources, Namibia) research trawl surveys in 2021 (Autumn and Summer surveys) and 2022 (Summer survey), with ethical clearance from Stellenbosch University (ACU-2022-26,954). Where available, metadata including size (TL), weight (g), sex (M/F), depth (m) and reproductive stage (maturity) were recorded during sample collection. As *M. paradoxus* lacks external sexual dimorphism, sex was routinely determined through dissection and visual inspection of the gonads during biological sampling.

2.2 | DNA Extraction, Library Preparation and Sequencing

Total DNA was extracted using the Qiagen DNeasy Blood and Tissue kit (Qiagen, Cape Town, South Africa) and was stored at −20°C. DNA quality and concentration were assessed using 2% agarose gel electrophoresis and quantified using the Qubit 4 Fluorometer with the dsDNA HS Assay (ThermoFisher Scientific, Massachusetts, United States). A subset of 20 samples was additionally run on the LabChip GX Touch 24 (PerkinElmer, Massachusetts, United States) to confirm integrity. Samples with a >1 mg total mass and >12.5 ng/mL concentration were selected for WGS.

Species identity was confirmed via PCR amplification of the mtDNA control region using species-specific primers (von der Heyden et al. 2007b). Products were visualized using 1% agarose gels.

Library preparation and 150 bp paired-end WGS re-sequencing were performed by BGI Genomics (Hong Kong) on a DBN-Seq platform. Samples were sequenced in two batches. Thirty-nine samples successfully passed QC and were sequenced.

2.3 | Sequence Filtering

Computations were performed using the University of Stellenbosch's HPC2: http://www.sun.ac.za/hpc. Quality checks of the raw reads were performed using FastQC v 0.11.5 (Andrews 2010) and MultiQC v 1.14 (Ewels et al. 2016). Reads were trimmed using Trimmomatic v 0.39 (Bolger et al. 2014) with parameters: MINLEN:40, HEADCROP:10, SLIDINGWINDOW:4:28. Read quality was confirmed using FastQC v 0.11.5 (Andrews 2010) and MultiQC v 1.14 (Ewels et al. 2016) before downstream analyses.

2.4 | Mapping and SNP Calling

Trimmed reads were mapped to the annotated and chromosome-level *Merluccius merluccius* genome (Martínez et al. 2024) using BWA-MEM v 0.7.13 (Li 2013). BAM files were filtered for a quality of 20, sorted, indexed and lastly merged by individual using SAMtools v 1.17 (Li et al. 2009). PCR duplicates were removed using Picard v 2.11.0 (https://broadinstitute.github.io/picard/). Overlapping reads were clipped using BamUtil v 2.02.2 (Jun et al. 2015). Depth of coverage was calculated using the depth tool in SAMtools v 1.17 (Li et al. 2009).

SNP calling was conducted using BCFtools v 1.19 (Danecek et al. 2021). SNPs were filtered using VCFtools v 0.1.17 (Danecek et al. 2011) to retain biallelic sites only (*–min-alleles 2* and *-max-alleles 2*); and removing indels (*–remove-indels*); low-quality SNPs (*–MinQ 30*); sites with missing data (*–max-missing 1*); minor allele count < 3 (*–mac 3*); depth < 8 (*-minDP 8*); fixed sites (*–max-non-ref-af 0*); heterozygosity ≧0.9 (*–hardy* and -exclude-positions) and individuals with more than 20% missing data. SNPs in the mtDNA scaffold (identified by COI alignment; Genbank accession number KX782995.1) were excluded (*–exclude-positions*).

2.5 | Population Structure and Genomic Differentiation

A principal component analysis (PCA) was performed using *dudi.pca* (*ade4* package; Dray and Dufour 2007) in R (R Core Team 2023; v 4.3.2). The analysis included all SNPs retained after filtering.

Distance-based redundancy analysis (dbRDA) was performed to examine relationships between genomic variation (SNP data) and biological and geographic variables. Predictor variables included depth (m), length (cm), weight (g), latitude, longitude, maturity, sex, collection year, collection month and sequencing batch. A dbRDA was performed using the *capscale* function (*vegan* package, Oksanen et al. 2025) in R. Multiple models were tested to evaluate the influence of different predictor sets. All predictor variables were included in the first full model. Thereafter, a correlation matrix was calculated in R, and variable combinations with Pearson correlation coefficient (r) greater than 0.8 or less than −0.8 were identified, and one variable from each pair was excluded. Variables that were not significant in the full model were removed in the reduced model. Some statistically significant variables, such as sequencing batch, were also excluded to focus on biologically meaningful predictors. To assess statistical significance, an ANOVA with 999 permutations was performed to test overall model significance and the contribution of individual predictor variables.

To assess whether missing data patterns could bias population or sex-based analyses, an identity-by-missingness (IBM) analysis was conducted in Plink v1.9 (--cluster-missing; Purcell et al. 2007). A pairwise distance matrix based on missing genotype patterns between individuals was compiled and used for multidimensional scaling (MDS). The first two MDS components were visualised in R using *ggplot2* with sample metadata such as sex, population and location overlaid to evaluate potential clustering.

Outlier SNPs were detected based on p-values derived from *pcadapt* (Privé et al. 2020) in R. Three correction methods were applied: q-value estimation (*qvalue*; Storey et al. 2023), Benjamini–Hochberg correction (*p.adjust*, *method* = *"BH"*) and Bonferroni correction (*p.adjust*, *method* = *"bonferroni"*). Loci with adjusted p-values below 0.1 were considered significant. SNPs identified using both the Benjamini–Hochberg and q-value estimation corrections were selected for downstream analysis, as these methods produced the same outlier SNPs. The Bonferroni correction was more stringent and was not used for downstream analysis, as its strict threshold can increase false negatives by excluding biologically relevant SNPs (Narum 2006).

Weighted Weir and Cockerham's F_{ST} was calculated across multiple comparisons: (1) among the four sampling locations, (2) between all males and females and (3) between males and females within the Core and East Edge sampling locations (excluding West Edge, where no male samples were available). Global weighted F_{ST} was computed using VCFtools v0.1.15 (*--weir-fst-pop*; Danecek et al. 2011). In addition, genome-wide F_{ST} was computed in non-overlapping 10 kb windows (--fst-window-size and *--fst-window-step*). This dataset was used to identify high-F_{ST} loci for subsequent gene ontology (GO) enrichment analysis (see below).

To classify selection, BayeScan v2.1 was used on genome-wide F_{ST} estimates (Foll and Gaggiotti 2008). SNPs with high posterior probabilities and positive alpha (α) values were classified as candidates for directional selection, while those with negative α values were indicative of balancing selection. The results were visualised using a plot of log10(q-value) against F_{ST}, allowing for identification of SNPs under selection after controlling for false discovery rate. The plotting method was adapted from Benestan et al. (2016).

To assess the linkage effects, analyses were repeated using LD pruned SNPs. SNPs in high LD ($r^2 > 0.2$) were filtered in 50 SNP sliding windows using Plink v2.0 (Chang et al. 2015; www.cog-genomics.org/plink/2.0/). This LD filtering step was conducted post hoc for validation purposes only and was not used for downstream analyses (with the exception of the Bayescan—which assumes SNP independence), as it can remove signals of local adaptation (Lotterhos and Whitlock 2015).

2.6 | Genomic Diversity and Inbreeding

Only SNPs located on mapped chromosomes were retained for genomic diversity and inbreeding analyses. Nucleotide diversity (π), Tajima's D (D), observed and expected heterozygosity (H_o; H_e) and the inbreeding coefficient were calculated for each individual and summarised by population and sex using VCFtools v0.1.15 (Danecek et al. 2011). Nucleotide diversity was calculated for each site (*--site-pi*) and both nucleotide diversity and Tajima's D were calculated in non-overlapping 50 kb windows (: *--window-pi* and *--window-pi-step*; *D*: *--TajimaD*). Observed and expected heterozygosity, and inbreeding coefficient (F_{IS}), were calculated (*--het*) and genome-wide observed heterozygosity was estimated (*--hardy*). The mean and standard error of these metrics was calculated separately for each location and sex in R.

Runs of homozygosity (ROH) were identified using BCFtools v1.19 (Narasimhan et al. 2016; *roh -AF-dflt 0.4 -G30*). A fixed allele frequency threshold of 0.4 was used since population-specific allele frequency data were unavailable. ROH density was calculated as the total number of ROH segments per 2 Mb bins for each population and sex. ROH were classified into three length categories: short ROH (< 20 kb), medium ROH (20–100 kb) and long ROH (> 100 kb). ROH counts per category were summed per individual in R and compared among populations and between sexes. The runs of homozygosity-based Inbreeding

Coefficient (F_{ROH}) was calculated as the ratio of total ROH length to the 715 Mb reference genome. Statistical comparisons were performed in R using the Shapiro–Wilk test for normality, Wilcoxon rank-sum test for sex comparisons and Kruskal–Wallis with Dunn's post hoc test (Bonferroni correction; *FSA* package; Ogle et al. 2025) for population comparisons and comparisons between ROH length categories. To formally assess the effects of sex, population and their interaction on F_{ROH}, we fitted generalized linear models using the *glmmTMB* package in R (McGillycuddy et al. 2025), with a beta error distribution and logit link. The West Edge population was excluded from this analysis due to the absence of male samples, which precluded testing the full *sex* × *population* interaction. Type III ANOVA (Wald chi-square tests; *car* package, Fox and Weisberg 2019) was used to evaluate the significance of fixed effects.

To reduce noise and highlight broad genome-wide trends when plotting, a rolling mean smoothing function and binning were applied in R (*zoo* package; Zeileis and Grothendieck 2005). Nucleotide diversity (π) and observed heterozygosity (H_o) were binned (50 kb windows), and smoothed ($k = 15$), Tajima's D values were binned (150 kb windows), and ROH density was smoothed ($k = 3$).

LD decay was first assessed across the genome, and more specifically within specific chromosomes containing regions of elevated F_{ST}, as well as within sample subsets, using PopLDdecay v3.42 (Zhang et al. 2019). The analysis was based on pairwise r^2 values from the original VCF (not filtered for LD; *-MAF* 0.05; *-MaxDist* 500). In addition, pairwise LD (r^2) was calculated using Plink v1.9 (Purcell et al. 2007; *–r² square*) for a subset of highly differentiated SNPs (50 kb intervals). Separate LD matrices were created for all individuals, as well as for each sex and region, to assess sex and region-specific linkage structure. LD matrices were visualised as heatmaps in R (*reshape2*: Wickham 2007; *ggplot2*: Wickham 2016).

2.7 | Gene Ontology Enrichment Analysis

High-F_{ST} SNPs (99th percentile; $F_{ST} = 0.428$) were extracted, and SNPs that were located within 200 kb of each other were grouped into regions. Genes and their corresponding Gene Ontology (GO) terms within these regions were extracted for GO enrichment analysis in R (*topGO* package; Alexa and Rahnenfuhrer 2023). GO annotations from the *M. merluccius* genome (Martínez et al. 2024) were used to construct a gene universe. Enriched GO terms were identified using a Fisher's exact test with *topGO*.

Enriched ($p < 0.01$) GO terms were classified into Primary and Secondary functional groups using QuickGO (Binns et al. 2009) to capture broad functional trends (primary categories) while retaining more specific biological functions (secondary categories).

To determine the genomic locations of enriched genes, significant GO terms were mapped to their corresponding genes in the annotated *M. merluccius* genome (Martínez et al. 2024). High-level (parent) GO terms that could not be directly mapped underwent a hierarchical refinement: child GO terms were retrieved using *GO.db* in R (*GOBOFFSPRING*; Carlson 2023), ensuring only directly annotated genes were retained. To improve specificity, parent GO terms with at least one significantly enriched child term were removed.

Significant GO terms were then intersected with those of genes located in high-F_{ST} regions, generating a candidate list. This approach prioritised genes most strongly associated with genomic divergence and reduced noise from broadly distributed GO terms.

3 | Results

3.1 | SNP Calling and Filtering

Thirty-nine *M. paradoxus* individuals were successfully sequenced and subjected to quality control and bioinformatic processing. All samples were confirmed as *M. paradoxus* as they amplified with the species-specific primers. Two samples were excluded based on a PCA, where they clustered separately from all other individuals along the first two axes, suggesting potential technical artefacts. This left 37 samples for downstream analyses. Sequencing depth ranged from 8× to 27.62× (mean coverage of 13.99×, SD = 3.92). Mapping rates averaged 95.89% (SD = 0.79), ranging from 94.80% to 97.70%. All properly paired reads were mapped, with reads detected across all 21 chromosomes. Of the 22,427,602 SNPs called, 2,347,710 were retained after filtering.

3.2 | Population Structure

Genome-wide variation was assessed using a PCA (Figure 2a), revealing clear genomic differentiation between sexes (PC1 = 4.67%), with males clustering tightly and females forming two loose groups. This split corresponds with spatial sex distributions: more males south of the spawning grounds off the West Coast and more females north, consistent across 2020 and 2021 (Figure S1).

This pattern was supported by dbRDA analyses, which found that sex significantly influenced genomic differentiation, more so than any other explanatory variable (Figure S2 and Table S2). The full dbRDA model was significant ($F = 9.452$, $p < 0.001$), explaining 80.616% of total variance. Sex was the strongest predictor ($F = 26.206$; $p < 0.001$), followed by latitude, maturity, longitude, sequencing batch, depth and length (all $p < 0.05$). Weight ($F = 0.014$, $p = 0.983$), month ($F = 0.073$, $p = 0.993$) and year ($F = 0.298$, $p = 0.726$) of sample collection were not significant and were removed from the reduced model.

Sequencing batch was significant ($F = 10.768$, $p < 0.001$) but did not cause clustering in the PCA, suggesting minimal impact on the observed differentiation (Figure S3a). Batches included both sexes, various maturities and locations (Figure S3a). As batch is a technical artifact, including it as a predictor could confound meaningful genomic patterns; therefore, it was excluded from the reduced model. Longitude and latitude ($r = -0.830$), and weight and length ($r = 0.912$) were highly correlated, so only longitude and length were retained. Depth of coverage did not explain PCA structure (Figure S3b). Most samples had medium coverage, while samples

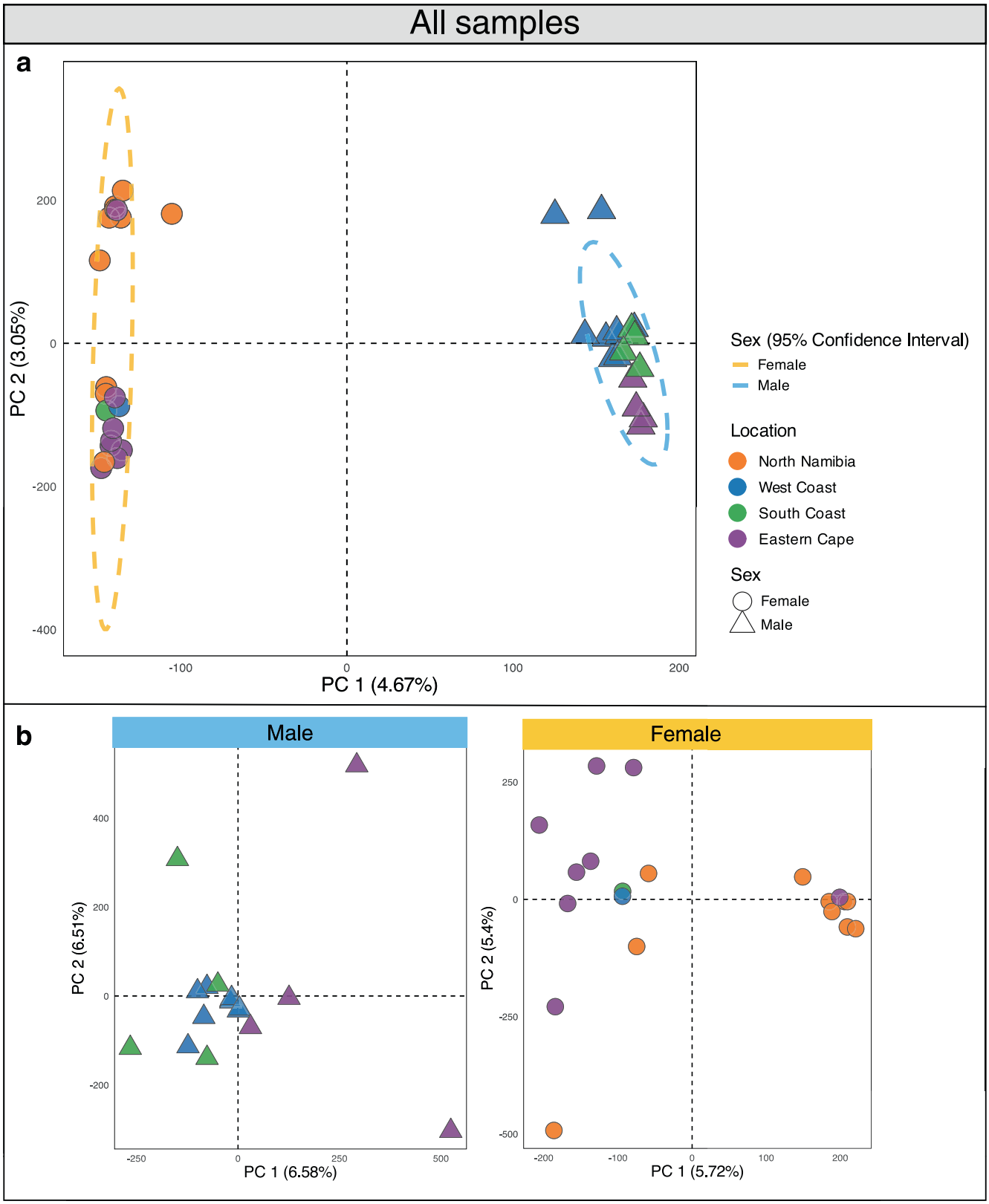

FIGURE 2 | Principal component analysis (PCA) of 2,347,710 SNP data for (a) all 37 *M. paradoxus* samples, (b) only male individuals and only female individuals from the southern African coastline. Each plot displays the first and second principal components. Individuals are colored by region, with sex denoted by point shape: circles represent females, and triangles represent males. A 95% confidence interval ellipse is drawn around male and female clusters to indicate group dispersion.

from Namibia and some from the West Coast had slightly lower coverage. No clear clustering was observed in the IBM analysis, indicating that patterns of missing data were not structured by sex or sampling location (Figure S4). This suggests that downstream analyses were unlikely to be biased by systematic missingness across biological or geographic groupings.

The final reduced model included sex, depth, length, longitude and maturity. It remained significant ($F = 21.018$, $p < 0.001$; Table S2 and Figure S2), explaining 77.221% of variance, with sex still the primary driver ($F = 34.956$, $p < 0.001$), while all retained explanatory variables were also significant.

Outlier detection using *pcadapt* identified 53,522 SNPs under selection using both *q*-values and the Benjamini-Hochberg (BH) procedure, and 34,368 SNPs under Bonferroni correction. SNPs identified using the BH and *q*-values procedures were selected for downstream analysis.

PCAs of outlier and neutral SNPs (Figure S5) showed that outlier SNPs reflected the global PCA with a strong, sex-driven split (PC1 = 61.43%; Figure S5a). In contrast, neutral SNPs showed minimal differentiation and a weak geographic pattern (Figure S5b). Individuals from the Core (West and South Coasts) were central, while individuals from the Eastern Cape (East Edge) clustered loosely to the left and those from North Namibia (West Edge) to the right, forming a weak east-to-west gradient.

Genomic differentiation was lowest between the West and South Coasts ($F_{ST} = -0.004$, $p < 0.001$; Table S3), suggesting minimal population structure. In addition, low genomic differentiation was also observed between the Eastern Cape and South Coast ($F_{ST} = -0.002$, $p < 0.001$; Table S3). Despite being the most geographically distant locations (~2700 km), North Namibia and the Eastern Cape exhibited unexpectedly low genomic differentiation ($F_{ST} = 0.001$, $p < 0.001$; Table S3). In contrast, North Namibia had higher F_{ST} values with the West Coast ($F_{ST} = 0.005$, $p < 0.001$; Table S3) and South Coast ($F_{ST} = 0.004$, $p < 0.001$; Table S3).

Based on these findings, locations were reorganised for downstream analyses: the West Coast and South Coast were merged into a single group (Core), while North Namibia and the Eastern Cape were renamed as West Edge and East Edge, respectively, reflecting their positions at the periphery of the species' range. Although F_{ST} values between the Eastern Cape and South Coast were low, the Eastern Cape was retained as a separate group as it covers the distribution range edge, is near a recorded spawning ground, and remains geographically distinct from the Core of the distribution. As sex better explained structure than geography, sex-specific results are emphasised. Region-specific analyses are provided in the Supporting Information but closely mirror the sex-based results, likely due to the strong spatial skew in sex ratios across the range.

Sex-based F_{ST} (0.008, $p < 0.001$) exceeded that between locations (Table S3). In the East Edge ($F_{ST} = 0.003$, $p < 0.001$), sex differentiation persisted but not in the Core ($F_{ST} = -0.013$, $p < 0.001$). This likely reflects sample imbalance (Core: 2 females, 13 males; East Edge: 4 females, 8 males). The East Edge results reinforce sex's influence and are a much more sex-representative region. Differentiation between Core and West Edge is likely due to sex imbalance (West Edge: only females). Similar patterns likely underlie East–West differentiation. Genome-wide F_{ST} revealed peaks on Chromosomes 1 and 2, suggesting sex-linked divergence (Figure 4a). These peaks are absent when comparing West Edge and East Edge females (Figure S6).

BayeScan was used to assess F_{ST} outliers on Chromosome 2, which showed the most consistent and extended region of elevated differentiation across analyses. Although Chromosome 1 also contained a high F_{ST} region, this was less pronounced than those on Chromosome 2. Among 58,100 SNPs tested on Chromosome 2, most showed low F_{ST} values and high *q*-values, consistent with neutrality. A subset showed high F_{ST} and low *q*-values, indicating diversifying selection ($q < 0.05$, $a > 0$; Figure S7). No SNPs were classified as being under balancing selection ($q < 0.05$, $a < 0$).

After LD pruning, 1,173,439 SNPs remained. PCA (Figure S8) and genome-wide F_{ST} showed the same sex differentiation and peaks on Chromosomes 1 and 2, confirming robustness.

3.3 | Genomic Diversity and Inbreeding

Diversity metrics were averaged by sex and region (Table S4). Mean nucleotide diversity (π) showed minimal variation. Tajima's D (D) was near zero in the Core ($D = -0.014$) and East Edge ($D = 0.016$), but notably lower in the West Edge ($D = -0.116$). Females had a slightly higher Tajima's D ($D = 0.148$) than males ($D = 0.073$).

Observed heterozygosity (H_o) exceeded expected heterozygosity (H_e), and inbreeding coefficients (F_{IS}) were negative in all groups, consistent with excess heterozygosity and low levels of inbreeding. F_{IS} was highest in the West Edge (−0.003) than in the Core ($F_{IS} = -0.062$) and East Edge ($F_{IS} = -0.065$). F_{ROH} was lowest in the West Edge ($F_{ROH} = 0.024$; Kruskal–Wallis test: $p = 0.22$; Figure S9). Males ($F_{ROH} = 0.033$) had a significantly higher F_{ROH} than females ($F_{ROH} = 0.023$; Wilcoxon rank-sum test: $p < 0.001$; Figure S9). Model-based tests confirmed a significant effect of sex (Type III ANOVA: $X^2 = 13.62$, df = 1, $p < 0.001$) but no significant effect of population (Type III ANOVA: $X^2 = 0.68$, df = 1, $p = 0.41$), nor any interaction between sex and population (Type III ANOVA: $X^2 = 0.17$, df = 1, $p = 0.68$). This suggests the sex difference was consistent across the Core and East Edge. Although the West Edge population was excluded from the model due to the absence of male samples, females from this region showed a wide range of F_{ROH} values (Figure S8).

Genome-wide diversity metrics were consistent across populations (Figures S10 and S11) and sexes (Figures 3 and 4). Regions on Chromosomes 1 and 2 showed notable differences in nucleotide diversity (π), Tajima's D (D), runs of homozygosity (ROH) and observed heterozygosity (H_o) in both sexes and populations. In Chromosome 2 (0.75–200.750 Mb), the Core had significantly lower ($=0.0004 \pm 0.0002$) than the West Edge ($=0.0009 \pm 0.0005$, $p < 0.001$) and East Edge ($=0.0008 \pm 0.0005$, $p < 0.001$; Figure S10a). This was coupled with a lower Tajima's D in the Core ($D = -0.7980 \pm 0.8110$), compared to the West ($D = 2.010 \pm 0.8930$, $p < 0.001$) and East Edges

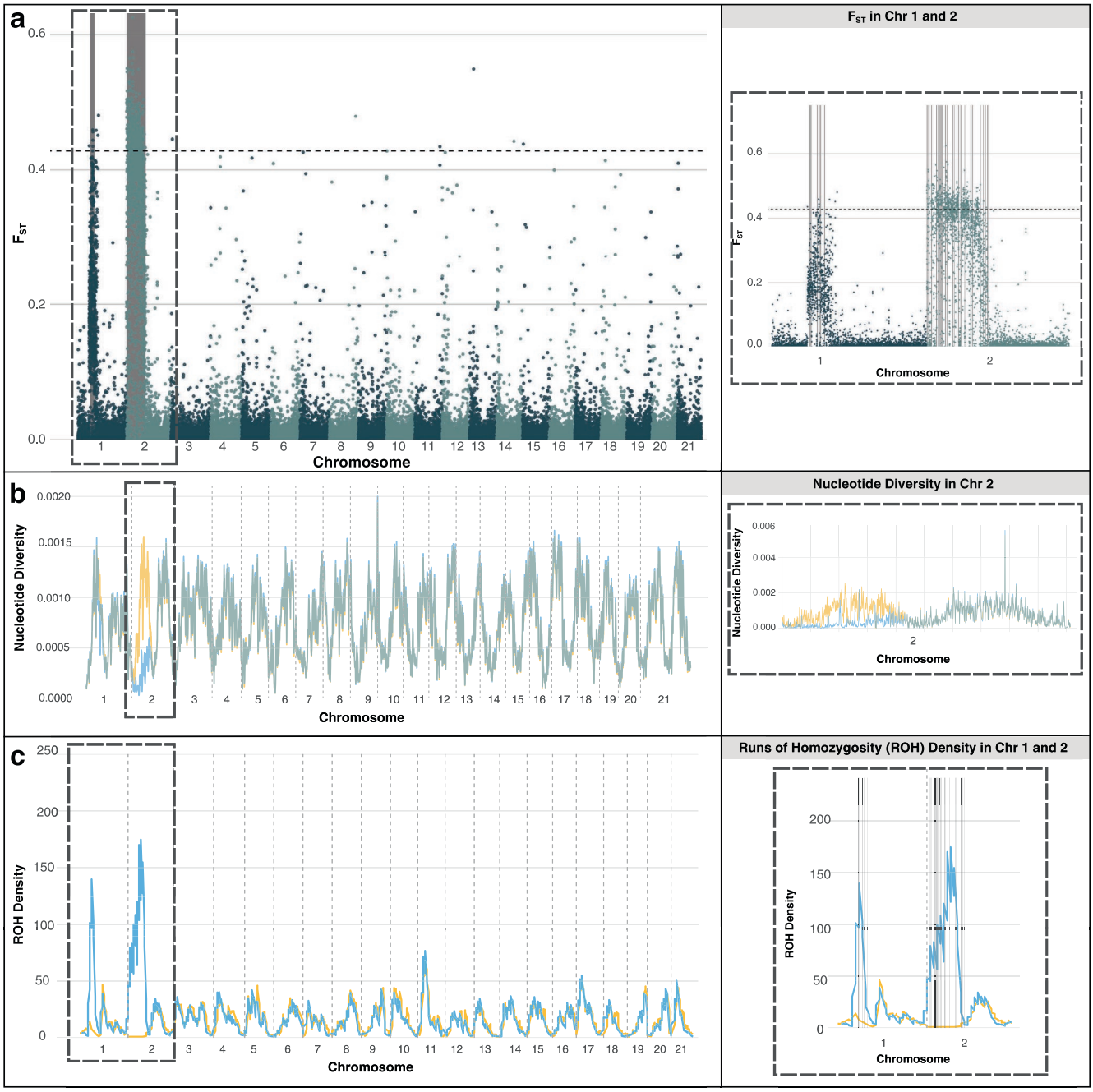

FIGURE 3 | Genome-wide (a) pairwise Weir and Cockerham F_{ST}, (b) nucleotide diversity (π) and (c) runs of homozygosity (ROH) density for male (blue) and female (yellow) *M. paradoxus* individuals, based on 2,347,710 SNPs. Chromosomes are separated by grey dashed lines on the x-axis. The right of each panel shows a zoomed-in view of chromosomes of interest, highlighting sex-specific genomic patterns. For (a), the horizontal grey dashed line marks the 99th percentile threshold, and grey-shaded regions indicate High-F_{ST} SNPs associated with enriched genes identified in the gene ontology (GO) enrichment analysis. Nucleotide diversity (π; b) was calculated in 50 kb windows, and ROH density (c) was calculated in 2 Mb bins along the genome.

($D = 1.7800 \pm 0.7250$, $p < 0.001$; Figure S11a). H_o in Chromosome 2 (0–22 Mb) was lower in the Core ($H_o = 0.2310 \pm 0.0929$), than in the West ($H_o = 0.6060 \pm 0.1490$, $p < 0.001$) and East Edges ($H_o = 0.4930 \pm 0.0773$, $p < 0.001$; Figure S11b). In contrast, ROH density was highest in the Core ($x^- = 114 \pm 80.7$) compared to the West ($x^- = 5$, $p < 0.05$) and East Edges ($x^- = 34.9 \pm 28.1$, $p < 0.05$; Figure S10b).

Sex differences in Chromosome 2 showed males had lower π (0.0003 ± 0.0002, $p < 0.001$; Figure 3b), Tajima's D ($D = 0.0170 \pm 0.8960$, $p < 0.001$), observed heterozygosity ($H_o = 0.1630 \pm 0.1300$, $p < 0.001$) and greater ROH density ($x^- = 81.9 \pm 70.3$, $p < 0.001$) than females ($\pi = 0.0009 \pm 0.0005$, $D = 2.6200 \pm 1.0400$; $H_o = 0.6340 \pm 0.1580$; $x^- = 0.2780 \pm 0.9740$; Figure 4).

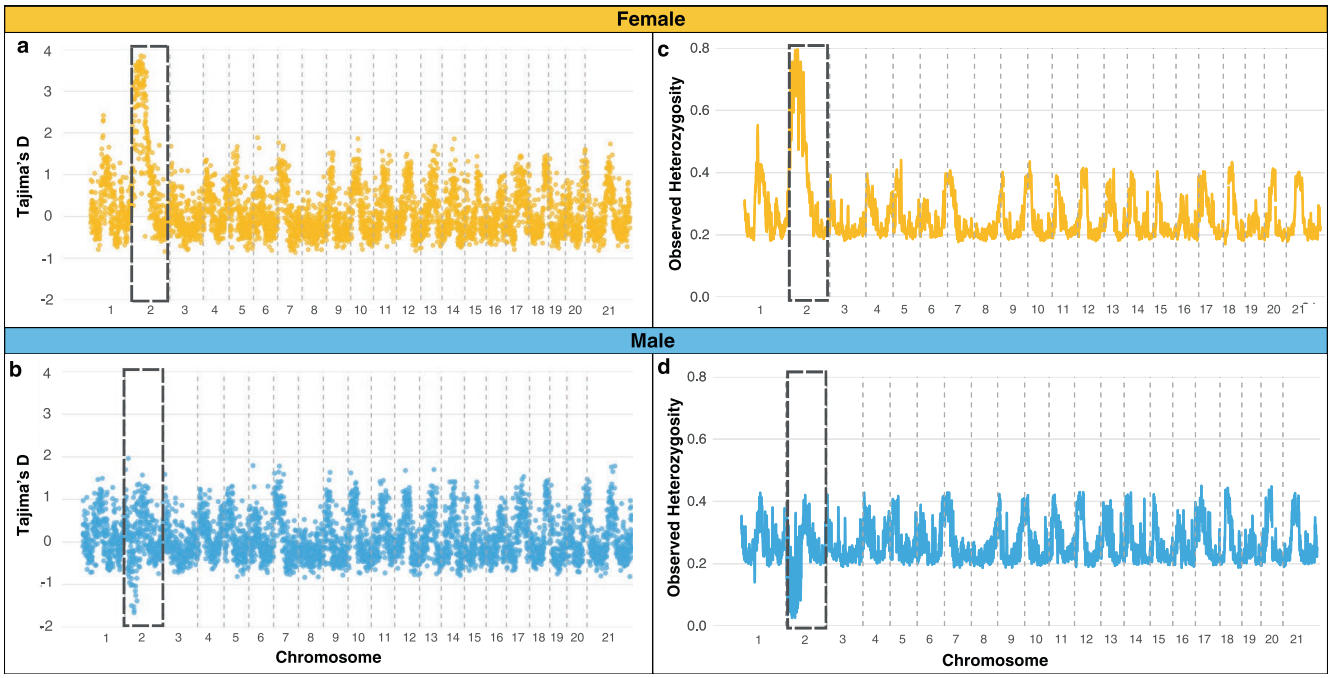

FIGURE 4 | Genome-wide Tajima's D (a, b) and observed heterozygosity (H_o; c, d) for *M. paradoxus*, based on 2,347,710 SNPs for each sex. Chromosomes are separated by grey dashed lines on the x-axis, with regions of interest highlighted by grey dashed boxes. Left panels show Tajima's D in 150 kb windows for females (yellow; a) and males (blue; b). Right panels show observed heterozygosity (per SNP, 50 kb windows) for females (yellow; c) and males (blue; d).

Another peak in Tajima's D was observed on Chromosome 1 (13.0–18.0 Mb) in females ($D = 0.9840 \pm 0.8020$) and the West Edge ($D = 0.7360 \pm 0.6800$). This differed from males ($D = 0.3530 \pm 0.5220$, $p < 0.001$; Figure 4a,c) and both the East Edge ($D = 0.8800 \pm 0.5590$; $p < 0.001$) and Core ($D = 0.0590 \pm 0.4360$; $p < 0.001$; Figure S11a). ROH density was also higher in males than in females in this region ($x^- = 60.9 \pm 55.6$ vs. $x^- = 3.83 \pm 7.26$, $p < 0.05$). Population differences here were not statistically significant ($p = 0.66$).

A total of 26,945 ROH segments were detected across all individuals. Short ROH were most frequent ($x^- = 431 \pm 108$), followed by medium ($x^- = 277 \pm 59$, $p < 0.001$) and long ($x^- = 20.2 \pm 15$, $p < 0.001$; Figure S12). Males had longer ROH ($x^- = 35.9 \pm 4.3$) than females ($x^- = 6.9 \pm 2.27$, $p < 0.05$; Figure S12), while no significant differences were found for short or medium ROH between sexes. Similarly, the Core population had significantly longer ROH ($x^- = 31.1 \pm 11.1$) than the West Edge ($x^- = 7.3 \pm 2.67$, $p < 0.05$; Figure S12). Short ROH were more frequent in the West Edge ($x^- = 504 \pm 68.3$) than in the Core ($x^- = 368 \pm 131$, $p < 0.05$; Figure S12).

Genome-wide LD decay followed the expected pattern, decaying rapidly within the first 10 kb and approaching baseline levels by 25 kb (Figure S13). LD decay was also calculated specifically for Chromosomes 1 and 2, where distinct regions of genomic differentiation were observed. Chromosome 1 exhibited a similar decay pattern to the genome-wide trend. On Chromosome 2, LD decayed more gradually overall, with r^2 values remaining above 0.1 over greater distances (Figure S13). However, when males and females were analysed separately, LD decayed more rapidly for each sex, with r^2 values dropping below 0.1 by approximately 25 kb (Figure S13).

Mean pairwise r^2 values for Chromosome 2 were visualised in heatmaps (Figure S14). The combined dataset (Figure S14a) showed a distinct block of high LD, indicating a cluster of non-randomly associated SNPs. When analysed by sex, this pattern is not present in the male or female datasets (Figure S14b,c). Males also showed more grey regions, reflecting low SNP variation, which prevents the calculation of r^2 for those positions.

3.4 | Gene Enrichment and Functional Analysis

High-F_{ST} SNPs ($n = 21{,}528$) were grouped into 244 regions, containing 1038 genes. These were used for GO enrichment analysis, which was performed using a gene universe of 15,029 genes and 4631 scored GO terms. Thirty-three GO terms (within 477 genes, $p < 0.01$) were found and classified into four primary and 11 secondary categories (Figure 5a). The primary categories included developmental processes, metabolic processes, cellular processes and stress responses. Developmental processes were most enriched ($n = 13$), further subdivided into organ development ($n = 5$) and neuronal process ($n = 8$).

Several of the most significant GO terms ($p < 0.005$) with a high gene count ($n > 5$) were related to developmental and cellular processes (Figure 5b). Within the stress response category, three genes were highly significant ($p < 0.0075$), and two genes had the highest gene ratio (gene ratio = 0.5), indicating strong enrichment. In contrast, the metabolic process category contained several less significant genes ($p < 0.001$) with a lower gene count ($n > 2.5$) compared to the other categories.

Enriched genes were filtered to retain only the genes that occurred within the regions on Chromosome 1 and 2 (High F_{ST}

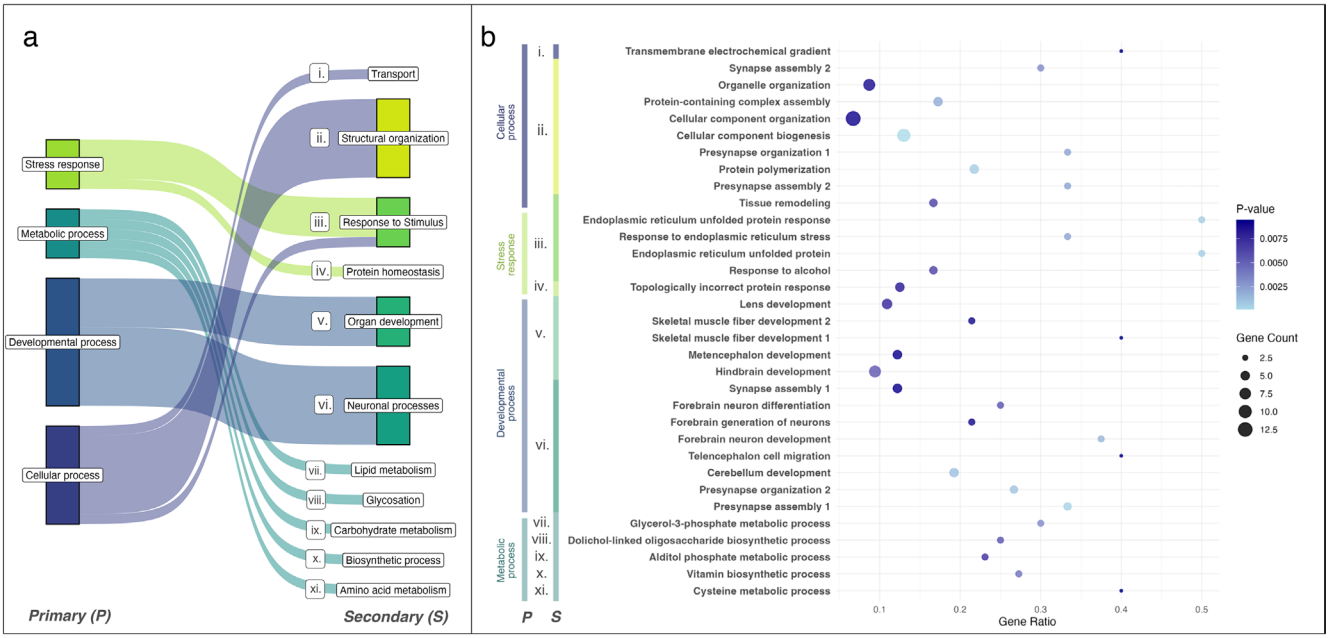

FIGURE 5 | Gene ontology (GO) enrichment results for genomic regions with high F_{ST} between males and females for 21,528 SNPs corresponding to 1038 genes. (a) Sankey plot summarising the 33 significantly enriched GO terms and their classification into primary and secondary functional groups. (b) Bubble plot displaying each significant GO term, where the x-axis represents the gene ratio (proportion of associated genes relative to the input genes), bubble size indicates gene count and colour intensity reflects statistical significance (*p*-value).

regions; Figure S15). This subset included three primary functional categories: developmental processes, cellular processes and metabolic processes.

Consistent with the broader gene enrichment results, the developmental process category was the most represented, particularly in relation to neuronal processes and organ development. Within organ development, three GO terms were retained: lens development in a camera-type eye (GO:0002088) and skeletal muscle fibre development (GO:0048743 and GO:0048742). Similarly, three GO terms related to neuronal processes were identified: synapse assembly (GO:0007416), cerebellum development (GO:0021549) and forebrain neuron development (GO:0021884).

The second most represented primary category was metabolic processes, which included two enriched GO terms: glycerol-3-phosphate metabolic process (GO:0006072), involved in lipid metabolism, and dolichol-linked oligosaccharide biosynthetic process (GO:0006488) associated with glycosylation.

The cellular process category included three GO terms: regulation of presynapse assembly (GO:1905606), positive regulation of synapse assembly (GO:0051965) and establishment or maintenance of transmembrane electrochemical gradient (GO:0010248).

4 | Discussion

Understanding patterns of genomic variation is crucial for the effective management of commercially exploited species, particularly those that span geo-political borders (Pinsky et al. 2018). In this study, we reveal that sex-based differentiation, rather than geographic structure, appears to be the principal driver of genomic variation in the commercially important deep-water hake (*M. paradoxus*) in southern Africa. Using WGS, we detected sex-associated divergence primarily concentrated on regions of Chromosomes 1 and 2. GO analyses suggest that rather than being linked to SD functions, these regions are associated with fundamental biological processes and traits likely essential for adaptation to environmental variability and, consequently, climate-driven range shifts. Our findings suggest that sex-specific selection, potentially linked to behavioural or environmental differences, may influence the spatial distribution of sexes in *M. paradoxus* and affect the species' future distribution, reproductive dynamics and resilience under changing ocean conditions.

4.1 | Sex-Linked Genomic Differentiation, Rather Than Geography, as the Primary Driver of Population Structure

Despite the highly heterogenous coastline of southern Africa, characterised by numerous disruptions to gene flow (Lett et al. 2024), genomic differentiation in *M. paradoxus* appears to be more strongly shaped by sex than geography. While horizontal environmental gradients appear limited across the mesopelagic range of *M. paradoxus* (200–1000 m; Burmeister 2001), surface waters where larvae occur (25–100 m; Grote et al. 2012), are subject to high environmental heterogeneity (Reygondeau et al. 2017; Robinson et al. 2010). *Merluccius* species, including *M. paradoxus*, exhibit diel vertical migration, moving upward at night and downward during the day in response to foraging opportunities and predator avoidance (Huse et al. 1998). This behaviour exposes individuals to fluctuating oxygen, light and temperature regimes, and may contribute to broad

environmental tolerance and enhanced capacity for dispersal in *M. paradoxus*, which could explain the weak geographic structure observed in this study (Okuda et al. 2014). Where female and male fishes differ in their responses to the environment, such ecological variation could also contribute to sex-associated genomic patterns as observed in our study.

To our knowledge, this study provides the first evidence of sex-associated genomic differentiation in the *Merluccius* genus that is not linked to known SD regions and is instead concentrated in autosomal regions (Martínez et al. 2024). Our findings contribute to a small but growing number of documented examples among marine teleosts where sex-specific divergence is not primarily associated with heteromorphic sex chromosomes (Barson et al. 2015; Wright et al. 2018). Notably, several studies describe systems in the early stage of sex chromosome evolution where divergence is beginning to accumulate around emerging SD regions in otherwise autosomal chromosomes (Kikuchi and Hamaguchi 2013; El Taher et al. 2021). The patterns in *M. paradoxus* described here appear to reflect sex-specific selection acting on autosomal regions not directly involved in sex determination, revealing a previously unrecognised layer of population structure in this commercially important, range-shifting species (von der Heyden et al. 2007a; Henriques et al. 2016; Forde et al. 2025).

Previously documented variation in sex ratios across the *M. paradoxus* distribution provides further support for underlying sex-linked population structure. Adult females are more commonly found in the western edge regions of the distribution, while males are more prevalent in the east, with more balanced sex ratios observed in the central areas where spawning is known to occur. While the sex composition of samples in this study was uneven in some locations, the overall patterns largely reflect known demographic trends; however, this was not fully captured in the east.

4.2 | Sex-Specific Divergence Maintained by Selection in Discrete Genomic Regions

To investigate the genomic basis of sex-linked differentiation, patterns of genome-wide diversity and divergence were assessed. Differentiation was concentrated in large regions on Chromosomes 1 and 2, with additional outlier SNPs found on Chromosomes 3, 8, 12, 14 and 15. Although overall genomic diversity was high and diversity metrics were generally consistent across populations and sexes, the regions on Chromosomes 1 and 2 showed pronounced differences in nucleotide diversity, ROH density, observed heterozygosity and Tajima's D. Several SNPs within these regions had F_{ST} values exceeding 0.4 (95th percentile), suggesting localised differentiation. Further analysis of the larger and more differentiated region on Chromosome 2 revealed evidence of sex-specific directional selection, including reduced nucleotide diversity and negative Tajima's D values in males, patterns consistent with a recent selective sweep (Wiberg et al. 2021). Additionally, males exhibited higher F_{ROH} and significantly longer (> 100 kb) ROH, further supporting this interpretation and potentially indicating a reduced effective population size (N_e) in males, although this would require further investigation (Shafer and Kardos 2025).

LD decay results indicate that the elevated LD signal on Chromosome 2 is driven by fixed or near-fixed differences between the sexes. When males and females were pooled, LD heatmaps showed a distinct region of elevated r^2 values in the differentiated region of Chromosome 2. This signal disappeared in sex-specific analyses, arguing against a structural rearrangement such as a large inversion, which typically leads to extended LD in one sex due to reduced recombination in heterozygotes (Martínez et al. 2024). Instead, results suggest divergent haplotypes maintained by sex-specific selection. Additionally, many SNPs in this region lacked r^2 values in males, likely due to reduced polymorphism, consistent with the region being nearly fixed in males, but more variable in females.

4.3 | Sex-Biased Selection in Response to Environmental Variability

Given that SD regions and structural rearrangements are unlikely drivers of population sub-structuring, sex-specific selection acting on physiological, behavioural, or reproductive traits (intrinsic factors; Ebel and Phillips 2016), shaped by environmental conditions (extrinsic factors; Reichard et al. 2014), or interactions between the two (De Lisle et al. 2018), provides possible explanations for the observed divergence between male and female *M. paradoxus*.

The two most differentiated regions in *M. paradoxus* are autosomes and do not contain key SD genes, such as *dmrt1*, *amh*, *cyp19ala* or *foxl2* (Nakamoto et al. 2009; Wu et al. 2010), and no enrichment of SD-related genes was detected genome-wide. While *SOX9-like* and *SOX8-like* genes—both involved in testis development and spermatogenesis—were present in the divergent region, their broad and multifunctional roles in development, lineage-specific retention and diversification and lack of enrichment make it unlikely that they function as master SD genes in *M. paradoxus* (Klüver et al. 2005; Voldoire et al. 2017; Yokoi et al. 2002). Moreover, the known master SD gene in the closely related *M. merluccius* (and reference genome for this study) is SRY-box transcription factor 3 (*sox3*), located on Chromosome 9 (Martínez et al. 2024; see also high mapping rates to the *M. merluccius* genome, supporting functional comparability and annotation reliability). Additionally, Martínez et al. (2024) reported evidence of sexual conflict in *M. merluccius*, with significant divergence between sexes on Chromosomes 5 and 12 in regions associated with olfactory-chemosensory communication and immune function (Martínez et al. 2024).

Although no evidence of a SD role was found in *M. paradoxus*, the diversity and high evolutionary turnover of SD systems (Kitano and Peichel 2012) across teleosts warrant consideration. Many teleost species lack distinct sex chromosomes and instead rely on polygenic or environmentally influenced sex determination (Liew et al. 2012; Vandeputte et al. 2007). For instance, sex determination is polygenic in Zebrafish (*Danio rerio*; Liew et al. 2012), European sea bass (*Dicentrarchus labrax*; Vandeputte et al. 2007), and African cichlid species (*Maylandia mbenjii* and *Astatotilapia burtoni*; Moore et al. 2022; Roberts et al. 2016). In some cases, such as in European sea bass (Vandeputte et al. 2007), Atlantic silverside (*Menidia menidia*; Conover and Kynard 1981) and the Nile Tilapia (*Oreochromis*

niloticus; Baroiller et al. 2009), sex determination is also temperature-sensitive, highlighting the flexibility and complexity of these systems. To date, the only *Merluccius* species with a characterised SD system is *M. merluccius* (XX/XY; Martínez et al. 2024), and polygenic or environmental SD systems have not been reported in this genus.

Spatial segregation of the sexes across the southern African coastline suggests that males and females not only occupy different parts of the species' range but may also be exposed to distinct environmental conditions such as oxygen availability, temperature, or regional differences in productivity (Hutchings et al. 2009; Shillington et al. 2006). Genes located in the highly differentiated regions on Chromosomes 1 and 2 were enriched for functions related to neuronal processes, skeletal muscle development and metabolic processes—traits that may influence behavioural or physiological responses to environmental variation. For instance, neuronal genes have been associated with variation in habitat use (Greenberg and Giller 2001; Pillans et al. 2021), mating behaviour (Pilastro et al. 2003; Tobler et al. 2011), and movement or migratory patterns (Pearse et al. 2019; as reviewed in Phillips et al. 2021). Similarly, skeletal muscle and metabolic genes may relate to differences in energetic demands (Somjee et al. 2022) or movement efficiency (Basolo and Alcaraz 2003). Divergence may also be shaped by intrinsic sex differences in reproductive investment (Lonn et al. 2017) or life history strategy (Barson et al. 2015). For example, females may invest more energy in egg production (Somjee et al. 2022) or undertake broader dispersal to suitable spawning habitats (Niella et al. 2022), while males may be more influenced by mate competition (Hutchings and Gerber 2002) or exhibit greater site fidelity (Jackson et al. 2024).

This pattern may also be shaped by sexual conflict involving sexually antagonistic alleles, where selection maintains genetic variants that benefit one sex but are deleterious or neutral to the other (Mank 2017). Such alleles are often located on autosomes and contribute to stable genomic divergence between sexes (Bonduriansky and Chenoweth 2009; Innocenti and Morrow 2010). In *M. paradoxus*, the fixation of divergent haplotypes in males but not females may represent such a signature. For example, in the tawny crazy ant (*Nylanderia fulva*), Eyer et al. (2019) showed that a set of autosomal alleles was selected differentially between males and females, while the remainder of the genome was randomly transmitted to the next generation. In their work, Eyer et al. (2019) showed that alleles at sex-specific loci were randomly inherited during egg development but selected differently at later developmental stages in each sex.

Regardless of how sex-specific selective pressures shape species and their populations, they can result in unique demographic patterns, including skewed sex ratios and spatial segregation between sexes. Supporting this interpretation, skewed sex ratios and sex-specific spatial distributions have been documented in several marine teleost species, including flounders (*Paralichthys* spp.; Luckenbach et al. 2009), Atlantic cod (*G. morhua*; Fevolden et al. 2015) and Greenland halibut (*Reinhardtius hippoglossoides*; Estévez-Barcia et al. 2025). Anthropogenic disturbances can also play a role; for example, an oil spill was reported to result in male-biased mortality and a subsequent skewed sex ratio in the gulf hake (*Urophycis cirrata*) and the southern hake (*Urophycis floridana*; Struch et al. 2019). In combination, these examples are among several that highlight the variety of ecological and biological processes that can generate or maintain sex-biased demographic patterns (De Lisle et al. 2018), similar to those observed here in *M. paradoxus*.

These findings are consistent with research in other *Merluccius* species, which show that sex-specific traits extend beyond reproduction and may contribute to ecological divergence. In both *M. merluccius* (Apostologamvrou et al. 2023; Philips 2014) and *M. paradoxus* (Botha 1986), females typically reach larger body sizes than males. However, Wilhelm et al. (2020) found that variation in otolith growth in *M. paradoxus* was primarily influenced by local environmental conditions (upwelling strength, chlorophyll concentration and sea surface temperature) rather than by sex and cohort. These findings suggest that the pronounced genomic divergence between sexes is unlikely to be explained by growth-related traits alone and instead may reflect selection associated with environmental pressures, or behavioural differences (Gardner et al. 2011). For example, male *M. merluccius* exhibit sexual dimorphism in drumming muscles, likely used for sound production during spawning (Groison et al. 2011), while sex differences in lipid content have been linked to metabolic activity, reproductive investment and adaptive responses to environmental changes, food availability and energetic demands (Panfili et al. 2024). Similarly, in the Argentinian hake (*M. hubbsi*), lower male growth rates have been associated with differences in white muscle fibre composition (Calvo 1989). Altogether, these examples suggest sex-specific environmental interactions and life history strategies may contribute to the observed sex-based genomic differentiation in *M. paradoxus*.

4.4 | Implications for a Shared Fishery in a Climate Change Hotspot

Sex-specific differences in distribution, genomic patterns and selection suggest that males and females may contribute differently to range dynamics and adaptive potential. This has important implications for the resilience and future structure of *M. paradoxus*.

Environmental changes in the southern African marine region, including east coast warming (Rouault et al. 2010), cooling on the south and west coasts (Blamey et al. 2015), shifts in upwelling regimes (Lamont et al. 2018) and expanding oxygen minimum zones (OMZs; Gilly et al. 2013), are expected to intensify regionally variable selective pressures. While surface ocean conditions are relatively well-studied (Garcia-Soto et al. 2021), mesopelagic responses remain poorly understood (St. John et al. 2016), particularly in ecologically complex and understudied regions like southern Africa (Blamey et al. 2015).

Gene enrichment patterns in females suggest potential adaptations to oxygen-poor and variable environments, which may contribute to their persistence in marginal or shifting habitats (Harts et al. 2014). Consistent with this, females at the range edges were more genomically similar to one another, despite occupying contrasting environments, than to individuals sampled in the centre (predominantly male). The West Edge is shaped by strong perennial upwelling and high productivity (Lamont

et al. 2018), while the East Edge experiences warmer, more stable conditions with localised, seasonal and less intense upwelling events (Hancke et al. 2023). These may exert distinct but parallel selection pressures favouring dispersal, metabolic plasticity and environmental tolerance. Although females were more prevalent in the west, sampled females from both edges exhibited elevated diversity and Tajima's D in differentiated regions. This pattern appears to be strongest on the western edge, where demographic and genomic signals align, though genomic signatures in females from the east also suggest a capacity for persistence and adaptation. Together, these findings support sex-specific differences in adaptive potential, with females, particularly those at the western edge, likely facilitating ongoing and future expansion.

Overall, our findings underscore the importance of incorporating sex-specific genomic patterns into studies of population structure and adaptive capacity. While current stock assessments account for sex at the population level, they do not capture the spatial and genomic variation revealed here. Disentangling how males and females differ in their genomic patterns, environmental tolerances and distributions could improve predictions of population dynamics and range expansions in *M. paradoxus*. Future research should prioritise identifying the mechanisms behind underlying sex differentiation in this species and assessing how these differences influence demographic resilience and connectivity under changing environmental conditions. More importantly, our results suggest that for marine species with well-documented geographically skewed sex ratios, sex differences need to be taken into consideration when investigating patterns of population structure and connectivity.

Author Contributions

Courtney E. C. Gardiner: data curation, formal analysis, investigation, methodology, visualization, writing – original draft, writing – review and editing. **Sophie von der Heyden:** conceptualization, funding acquisition, methodology, project administration, resources, supervision, writing – review and editing. **Conrad A. Matthee:** resources, writing – review and editing. **Einar E. Nielsen:** conceptualization, funding acquisition, methodology, project administration, writing – review and editing. **José M. Pujolar:** data curation, methodology, writing – review and editing. **Rita Castilho:** conceptualization, funding acquisition, writing – review and editing. **Regina L. Cunha:** writing – review and editing. **Joana I. Robalo:** conceptualization, funding acquisition, writing – review and editing. **Deon Durholtz:** resources, writing – review and editing. **Tracey P. Fairweather:** visualization, writing – review and editing. **Johannes N. Kathena:** resources, writing – review and editing. **Romina Henriques:** conceptualization, funding acquisition, methodology, project administration, resources, supervision, writing – review and editing.

Acknowledgements

This work was supported by a Biodiversa+ BiodivClim 2020 grant. BioDivClim Grant number 0156-00018B Innovation Fund Denmark (BiodivERsA call 2019-2020) and by the Department of Science and Innovation (DSI), South Africa for the project "Biodiversity on the run: evolutionary and socio-economic consequences of shifting distribution ranges in commercially exploited marine fishes". J.I.R. was supported by the FCT—Foundation for Science and Technology, projects MARE/UIDB/MAR/04292, MARE/UIDP/04292 and LA/P/0069/2020 granted to MARE and ARNET. R.C. and R.L.C. received Portuguese national funds from FCT—Foundation for Science and Technology through projects UIDB/04326/2020, UIDP/04326/2020 and LA/P/0101/2020. We thank the South African Department of Forestry, Fisheries and the Environment (DFFE), CapMarine and Namibian Ministry of Fisheries and Marine Resources (MFMR) for providing *Merluccius paradoxus* samples and for sharing their valuable insights. We are also grateful to Dr. Kelvin Hull and Dr. Andrew Ndhlovu for their thoughtful discussion and helpful suggestions throughout the course of this research. Thanks also to Stellenbosch University's High Performance Computing cluster for hosting the raw data and facilitating computationally intensive analyses, and to Gerhard Van Wageningen for his assistance with cluster access and troubleshooting. The authors declare no conflict of interest in this research.

Conflicts of Interest

The authors declare no conflicts of interest.

Data Availability Statement

The raw genomic data that support the findings of this study are openly available in GenBank at BioProject:PRJNA1336109, and the sample metadata is available in Zenodo at https://doi.org/10.5281/zenodo.17241831.

References

Alexa, A., and J. Rahnenfuhrer. 2023. "*topGO*: Enrichment Analysis for Gene Ontology (Version 2.54.0) [R Package]. Bioconductor." https://bioconductor.org/packages/topGO https://doi.org/10.18129/B9.bioc.topGO.

Andrews, S. 2010. "FastQC: A Quality Control Tool for High Throughput Sequence Data [Online]." http://www.bioinformatics.babraham.ac.uk/projects/fastqc/.

Apostologamvrou, C., M. Vlachou, A. Theocharis, C. Ntavaros, and D. Klaoudatos. 2023. "Reproductive Aspects of European Hake, (*Merluccius merluccius*, Linnaeus, 1758) Based on Histological Depiction of Both Sexes in the Eastern Mediterranean (Aegean Sea)." *Regional Studies in Marine Science* 68: 103281. https://doi.org/10.1016/j.rsma.2023.103281.

Baroiller, J. F., H. D'Cotta, E. Bezault, S. Wessels, and G. Hoerstgen-Schwark. 2009. "Tilapia Sex Determination: Where Temperature and Genetics Meet." *Comparative Biochemistry and Physiology Part A: Molecular & Integrative Physiology* 153, no. 1: 30–38. https://doi.org/10.1016/j.cbpa.2008.11.018.

Barson, N. J., T. Aykanat, K. Hindar, et al. 2015. "Sex-Dependent Dominance at a Single Locus Maintains Variation in Age at Maturity in Salmon." *Nature* 528, no. 7582: 405–408. https://doi.org/10.1038/nature16062.

Basolo, A. L., and G. Alcaraz. 2003. "The Turn of the Sword: Length Increases Male Swimming Costs in Swordtails." *Proceedings of the Royal Society of London. Series B: Biological Sciences* 270, no. 1524: 1631–1636. https://doi.org/10.1098/rspb.2003.2388.

Baudron, A. R., T. Brunel, M.-A. Blanchet, et al. 2020. "Changing Fish Distributions Challenge the Effective Management of European Fisheries." *Ecography* 43, no. 4: 494–505. https://doi.org/10.1111/ecog.04864.

Beaudry-Sylvestre, M., H. P. Benoît, and J. A. Hutchings. 2022. "Combined Effects of Exploitation and Environmental Change on Life History: A Comparative Analysis on Atlantic Herring." *ICES Journal of Marine Science* 79, no. 10: 2728–2740. https://doi.org/10.1093/icesjms/fsac209.

Belton, B., and S. H. Thilsted. 2014. "Fisheries in Transition: Food and Nutrition Security Implications for the Global South." *Global Food Security* 3, no. 1: 59–66. https://doi.org/10.1016/j.gfs.2013.10.001.

Benestan, L., B. K. Quinn, H. Maaroufi, et al. 2016. "Seascape Genomics Provides Evidence for Thermal Adaptation and Current-Mediated

Population Structure in American Lobster (*Homarus americanus*)." *Molecular Ecology* 25, no. 20: 5073–5092. https://doi.org/10.1111/mec.13811.

Binns, D., E. Dimmer, R. Huntley, D. Barrell, C. O'Donovan, and R. Apweiler. 2009. "QuickGO: A Web-Based Tool for Gene Ontology Searching." *Bioinformatics* 25, no. 22: 3045–3046. https://doi.org/10.1093/bioinformatics/btp536.

Blamey, L. K., L. J. Shannon, J. J. Bolton, et al. 2015. "Ecosystem Change in the Southern Benguela and the Underlying Processes." *Journal of Marine Systems* 144: 9–29. https://doi.org/10.1016/j.jmarsys.2014.11.006.

Bolger, A. M., M. Lohse, and B. Usadel. 2014. "Trimmomatic: A Flexible Trimmer for Illumina Sequence Data." *Bioinformatics* 30, no. 15: 2114–2120. https://doi.org/10.1093/bioinformatics/btu170.

Bonduriansky, R., and S. F. Chenoweth. 2009. "Intralocus Sexual Conflict." *Trends in Ecology & Evolution* 24, no. 5: 280–288. https://doi.org/10.1016/j.tree.2008.12.005.

Bors, E. K., S. Herrera, J. A. Morris Jr., and T. M. Shank. 2019. "Population Genomics of Rapidly Invading Lionfish in the Caribbean Reveals Signals of Range Expansion in the Absence of Spatial Population Structure." *Ecology and Evolution* 9, no. 6: 3306–3320. https://doi.org/10.1002/ece3.4952.

Botha, L. 1986. "Reproduction, Sex Ratio and Rate of Natural Mortality of Cape Hakes *Merluccius capensis* Cast. and *M. paradoxus* Franca in the Cape of Good Hope Area." *South African Journal of Marine Science* 4: 23–35. https://doi.org/10.2989/025776186784461783.

Burmeister, L.-M. 2001. "Depth-Stratified Density Estimates and Distribution of the Cape Hake *Merluccius Capensis* and *M. Paradoxus* Off Namibia Deduced From Survey Data, 1990–1999." *South African Journal of Marine Science* 23, no. 1: 347–356. https://doi.org/10.2989/025776101784528863.

Calvo, J. 1989. "Sexual Differences in the Increase of White Muscle Fibres in Argentine Hake, *Merluccius hubbsi*, From the San Matias Gulf (Argentina)." *Journal of Fish Biology* 35, no. 2: 207–214. https://doi.org/10.1111/j.1095-8649.1989.tb02970.x.

Carlson, M. 2023. "*GO.db*: A Set of Annotation Maps Describing the Entire Gene Ontology. R Package Version 3.18.0."

Chang, C. C., C. C. Chow, L. C. Tellier, S. Vattikuti, S. M. Purcell, and J. J. Lee. 2015. "Second-Generation PLINK: Rising to the Challenge of Larger and Richer Datasets." *GigaScience* 4, no. 1: s13742-015. https://doi.org/10.1186/s13742-015-0047-8.

Conover, D. O., and B. E. Kynard. 1981. "Environmental Sex Determination: Interaction of Temperature and Genotype in a Fish." *Science* 213, no. 4507: 577–579. https://doi.org/10.1126/science.213.4507.577.

Dalongeville, A., E. S. Nielsen, P. R. Teske, and S. von der Heyden. 2022. "Comparative Phylogeography in a Marine Biodiversity Hotspot Provides Novel Insights Into Evolutionary Processes Across the Atlantic-Indian Ocean Transition." *Diversity and Distributions* 28: 2622–2636. https://doi.org/10.1111/ddi.13534.

Danecek, P., A. Auton, G. Abecasis, et al. 2011. "The Variant Call Format and VCFtools." *Bioinformatics* 27, no. 15: 2156–2158. https://doi.org/10.1093/bioinformatics/btr330.

Danecek, P., J. K. Bonfield, J. Liddle, et al. 2021. "Twelve Years of SAMtools and BCFtools." *GigaScience* 10, no. 2: giab008. https://doi.org/10.1093/gigascience/giab008.

De Lisle, S. P., D. Goedert, A. M. Reedy, and E. I. Svensson. 2018. "Climatic Factors and Species Range Position Predict Sexually Antagonistic Selection Across Taxa." *Philosophical Transactions of the Royal Society, B: Biological Sciences* 373, no. 1757: 20170415. https://doi.org/10.1098/rstb.2017.0415.

DFFE (Department of Forestry, Fisheries and the Environment). 2023. *Status of the South African Marine Fishery Resources 2023*. DFFE.

Dray, S., and A. Dufour. 2007. "The *ade4* Package: Implementing the Duality Diagram for Ecologists." *Journal of Statistical Software* 22, no. 4: 1–20. https://doi.org/10.18637/jss.v022.i04.

Dudaniec, R. Y., C. J. Yong, L. T. Lancaster, E. I. Svensson, and B. Hansson. 2018. "Signatures of Local Adaptation Along Environmental Gradients in a Range-Expanding Damselfly (*Ischnura elegans*)." *Molecular Ecology* 27, no. 11: 2576–2593. https://doi.org/10.1111/mec.14709.

Ebel, E. R., and P. C. Phillips. 2016. "Intrinsic Differences Between Males and Females Determine Sex-Specific Consequences of Inbreeding." *BMC Evolutionary Biology* 16, no. 1: 36. https://doi.org/10.1186/s12862-016-0604-5.

Eklund, A. M., and T. E. Targett. 1990. "Reproductive Seasonality of Fishes Inhabiting Hard Bottom Areas in the Middle Atlantic Bight." *Copeia* 1990, no. 4: 1180–1184. https://doi.org/10.2307/1446512.

El Taher, A., F. Ronco, M. Matschiner, W. Salzburger, and A. Böhne. 2021. "Dynamics of Sex Chromosome Evolution in a Rapid Radiation of Cichlid Fishes." *Science Advances* 7, no. 36: eabe8215. https://doi.org/10.1126/sciadv.abe8215.

Engelhard, G. H., D. A. Righton, and J. K. Pinnegar. 2014. "Climate Change and Fishing: A Century of Shifting Distribution in North Sea Cod." *Global Change Biology* 20, no. 8: 2473–2483. https://doi.org/10.1111/gcb.12513.

Estévez-Barcia, D., D. Roy, M. Vihtakari, et al. 2025. "Sex Influences the Genetic Structure of Greenland Halibut in the North Atlantic." *Ecology and Evolution* 15, no. 2: e70822. https://doi.org/10.1002/ece3.70822.

Ewels, P., M. Magnusson, S. Lundin, and M. Käller. 2016. "MultiQC: Summarize Analysis Results for Multiple Tools and Samples in a Single Report." *Bioinformatics* 32, no. 19: 3047–3048. https://doi.org/10.1093/bioinformatics/btw354.

Eyer, P.-A., A. J. Blumenfeld, and E. L. Vargo. 2019. "Sexually Antagonistic Selection Promotes Genetic Divergence Between Males and Females in an Ant." *Proceedings of the National Academy of Sciences* 116, no. 48: 24157–24163. https://doi.org/10.1073/pnas.1906568116.

Fevolden, S.-E., J.-I. Westgaard, and T. Pedersen. 2015. "Extreme Male-Skewed Sex Ratios on Spawning Grounds for Atlantic Cod (*Gadus morhua*) With Typical Coastal Cod Signatures of the *Pan I* (Pantophysin) Locus." *Sexuality and Early Development in Aquatic Organisms* 1, no. 2: 133–142. https://doi.org/10.3354/sedao00013.

Fifer, J. E., N. Yasuda, T. Yamakita, C. B. Bove, and S. W. Davies. 2022. "Genetic Divergence and Range Expansion in a Western North Pacific Coral." *Science of the Total Environment* 813: 152423. https://doi.org/10.1016/j.scitotenv.2021.152423.

Foll, M., and O. Gaggiotti. 2008. "A Genome-Scan Method to Identify Selected Loci Appropriate for Both Dominant and Codominant Markers: A Bayesian Perspective." *Genetics* 180, no. 2: 977–993. https://doi.org/10.1534/genetics.108.092221.

Forde, S., S. von der Heyden, A. Le Moan, et al. 2025. "Management and Conservation Implications of Cryptic Population Substructure for Two Commercially Exploited Fishes (*Merluccius* spp.) in Southern Africa." *Molecular Ecology Resources* 25: e13820. https://doi.org/10.1111/1755-0998.13820.

Fox, J., and S. Weisberg. 2019. *An R Companion to Applied Regression*. Third ed. Sage. https://www.john-fox.ca/Companion/.

Gandra, M., J. Assis, M. R. Martins, and D. Abecasis. 2021. "Reduced Global Genetic Differentiation of Exploited Marine Fish Species." *Molecular Biology and Evolution* 38, no. 4: 1402–1412. https://doi.org/10.1093/molbev/msaa299.

García Molinos, J., H. L. Hunt, M. E. Green, C. Champion, J. R. Hartog, and G. T. Pecl. 2022. "Climate, Currents and Species Traits Contribute to Early Stages of Marine Species Redistribution." *Communications Biology* 5, no. 1: 1–10. https://doi.org/10.1038/s42003-022-04273-0.

Garcia-Soto, C., L. Cheng, L. Caesar, et al. 2021. "An Overview of Ocean Climate Change Indicators: Sea Surface Temperature, Ocean Heat Content, Ocean pH, Dissolved Oxygen Concentration, Arctic Sea Ice Extent, Thickness and Volume, Sea Level and Strength of the AMOC (Atlantic Meridional Overturning Circulation)." *Frontiers in Marine Science* 8: 642372. https://doi.org/10.3389/fmars.2021.642372.

Gardner, J. L., A. Peters, M. R. Kearney, L. Joseph, and R. Heinsohn. 2011. "Declining Body Size: A Third Universal Response to Warming?" *Trends in Ecology & Evolution* 26, no. 6: 285–291. https://doi.org/10.1016/j.tree.2011.03.005.

Gilly, W. F., J. M. Beman, S. Y. Litvin, and B. H. Robison. 2013. "Oceanographic and Biological Effects of Shoaling of the Oxygen Minimum Zone." *Annual Review of Marine Science* 5, no. 1: 393–420. https://doi.org/10.1146/annurev-marine-120710-100849.

Greenberg, L. A., and P. S. Giller. 2001. "Individual Variation in Habitat Use and Growth of Male and Female Brown Trout." *Ecography* 24, no. 2: 212–224. https://doi.org/10.1034/j.1600-0587.2001.240212.x.

Groison, A.-L., O. S. Kjesbu, and M. Suquet. 2011. "Sexual Dimorphism of Drumming Muscles in European Hake (*Merluccius merluccius*)." *Environmental Biology of Fishes* 91, no. 1: 7–13. https://doi.org/10.1007/s10641-010-9753-3.

Grote, B., E. Stenevik, W. Ekau, H. Verheye, M. Lipiński, and W. Hagen. 2012. "Spawning Strategies and Transport of Early Stages of the Two Cape Hake Species, *Merluccius paradoxus* and *M. capensis*, in the Southern Benguela Upwelling System." *African Journal of Marine Science* 34, no. 2: 195–204. https://doi.org/10.2989/1814232X.2012.675040.

Hancke, L., D. Smeed, M. Roberts, C. Russo, D. Rayner, and F. Jebri. 2023. "Atmospheric and Advective Forcing of Upwelling on South Africa's Central Agulhas Bank." *Deep Sea Research Part II: Topical Studies in Oceanography* 209: 105293. https://doi.org/10.1016/j.dsr2.2023.105293.

Harts, A. M. F., L. E. Schwanz, and H. Kokko. 2014. "Demography Can Favour Female-Advantageous Alleles." *Proceedings of the Royal Society B: Biological Sciences* 281, no. 1790: 20140005. https://doi.org/10.1098/rspb.2014.0005.

Hastings, R. A., L. A. Rutterford, J. J. Freer, R. A. Collins, S. D. Simpson, and M. J. Genner. 2020. "Climate Change Drives Poleward Increases and Equatorward Declines in Marine Species." *Current Biology* 30, no. 8: 1572–1577.e2. https://doi.org/10.1016/j.cub.2020.02.043.

Henriques, R., W. Potts, W. Sauer, and P. Shaw. 2012. "Evidence of Deep Genetic Divergence Between Populations of an Important Recreational Fishery Species, *Lichia amia* L. 1758, Around Southern Africa." *African Journal of Marine Science* 34, no. 4: 585–591. https://doi.org/10.2989/1814232X.2012.749809.

Henriques, R., S. von der Heyden, M. R. Lipinski, et al. 2016. "Spatio-Temporal Genetic Structure and the Effects of Long-Term Fishing in Two Partially Sympatric Offshore Demersal Fishes." *Molecular Ecology* 25, no. 23: 5843–5861. https://doi.org/10.1111/mec.13890.

Hirao, A. S., J. Imoto, A. Fujiwara, et al. 2024. "Genome-Wide SNP Analysis Coupled With Geographic and Reproductive-Phenological Information Reveals Panmixia in a Classical Marine Species, the Japanese Jack Mackerel (*Trachurus japonicus*)." *Fisheries Research* 279: 107146. https://doi.org/10.1016/j.fishres.2024.107146.

Hobday, A. J., and G. T. Pecl. 2014. "Identification of Global Marine Hotspots: Sentinels for Change and Vanguards for Adaptation Action." *Reviews in Fish Biology and Fisheries* 24, no. 2: 415–425. https://doi.org/10.1016/j.pocean.2009.07.046.

Huse, I., H. Hamukuaya, D. C. Boyer, P. E. Malan, and T. Strømme. 1998. "The Diurnal Vertical Dynamics of Cape Hake and Their Potential Prey." *South African Journal of Marine Science* 19, no. 1: 365–376. https://doi.org/10.2989/025776198784126746.

Hutchings, J. A., and L. Gerber. 2002. "Sex–Biased Dispersal in a Salmonid Fish." *Proceedings of the Royal Society of London, Series B: Biological Sciences* 269, no. 1508: 2487–2493. https://doi.org/10.1098/rspb.2002.2176.

Hutchings, L., C. D. Van der Lingen, L. J. Shannon, et al. 2009. "The Benguela Current: An Ecosystem of Four Components." *Progress in Oceanography* 83, no. 1–4: 15–32. https://doi.org/10.1016/j.pocean.2009.07.046.

Innocenti, P., and E. H. Morrow. 2010. "The Sexually Antagonistic Genes of *Drosophila melanogaster*." *PLoS Biology* 8, no. 3: e1000335. https://doi.org/10.1371/journal.pbio.1000335.

Jackson, J. R., G. R. Jacobs, A. W. Latzka, T. Landsman, B. P. Young, and A. R. McCune. 2024. "Spawning Migration, Sex-Specific Home Ranges, and Seasonal Site Fidelity in a Lacustrine Population of Bowfin (*Amia ocellicauda*)." *Environmental Biology of Fishes* 107, no. 12: 1369–1388. https://doi.org/10.1007/s10641-024-01585-4.

Jacobs, A., M. Carruthers, R. Eckmann, et al. 2019. "Rapid Niche Expansion by Selection on Functional Genomic Variation After Ecosystem Recovery." *Nature Ecology & Evolution* 3, no. 1: 77–86. https://doi.org/10.1038/s41559-018-0742-9.

Jansen, T., P. Kainge, L. Singh, et al. 2015. "Spawning Patterns of Shallow-Water Hake (*Merluccius capensis*) and Deep-Water Hake (*M. paradoxus*) in the Benguela Current Large Marine Ecosystem Inferred From Gonadosomatic Indices." *Fisheries Research* 172: 168–180. https://doi.org/10.1016/j.fishres.2015.07.009.

Jiménez-Mena, B., A. Le Moan, A. Christensen, et al. 2019. "Weak Genetic Structure Despite Strong Genomic Signal in Lesser Sandeel in the North Sea." *Evolutionary Applications* 13, no. 2: 376–387. https://doi.org/10.1111/eva.12875.

Jose, A., S. Sukumaran, S. K. Roul, et al. 2023. "Genetic Analyses Reveal Panmixia in Indian Waters and Population Subdivision Across Indian Ocean and Indo-Malay Archipelago for *Decapterus russelli*." *Scientific Reports* 13, no. 1: 22860. https://doi.org/10.1038/s41598-023-49805-8.

Jun, G., M. K. Wing, G. R. Abecasis, and H. M. Kang. 2015. "An Efficient and Scalable Analysis Framework for Variant Extraction and Refinement From Population-Scale DNA Sequence Data." *Genome Research* 25, no. 6: 918–925. https://doi.org/10.1101/gr.176552.114.

Kikuchi, K., and S. Hamaguchi. 2013. "Novel Sex-Determining Genes in Fish and Sex Chromosome Evolution." *Developmental Dynamics* 242, no. 4: 339–353. https://doi.org/10.1002/dvdy.23927.

Kitano, J., and C. L. Peichel. 2012. "Turnover of Sex Chromosomes and Speciation in Fishes." *Environmental Biology of Fishes* 94, no. 3: 549–558. https://doi.org/10.1007/s10641-011-9853-8.

Klüver, N., M. Kondo, A. Herpin, H. Mitani, and M. Schartl. 2005. "Divergent Expression Patterns of *Sox9* Duplicates in Teleosts Indicate a Lineage Specific Subfunctionalization." *Development Genes and Evolution* 215, no. 6: 297–305. https://doi.org/10.1007/s00427-005-0477-x.

Kuparinen, A., J. A. Hutchings, and R. S. Waples. 2016. "Harvest-Induced Evolution and Effective Population Size." *Evolutionary Applications* 9, no. 5: 658–672. https://doi.org/10.1111/eva.12373.

Lamont, T., M. García-Reyes, S. J. Bograd, C. D. van der Lingen, and W. J. Sydeman. 2018. "Upwelling Indices for Comparative Ecosystem Studies: Variability in the Benguela Upwelling System." *Journal of Marine Systems* 188: 3–16. https://doi.org/10.1016/j.jmarsys.2017.05.007.

Lett, C., B. S. Malauene, T. B. Hoareau, D. M. Kaplan, and F. Porri. 2024. "Corridors and Barriers to Marine Connectivity Around Southern Africa." *Marine Ecology Progress Series* 731: 105–127. https://doi.org/10.3354/meps14312.

Li, H. 2013. "Aligning Sequence Reads, Clone Sequences and Assembly Contigs With BWA-MEM." arXiv:13033997. http://arxiv.org/abs/1303.3997.

Li, H., B. Handsaker, A. Wysoker, et al. 2009. "The Sequence Alignment/Map Format and SAMtools." *Bioinformatics* 25, no. 16: 2078–2079. https://doi.org/10.1093/bioinformatics/btp352.

Liew, W. C., R. Bartfai, Z. Lim, R. Sreenivasan, K. R. Siegfried, and L. Orban. 2012. "Polygenic Sex Determination System in Zebrafish." *PLoS One* 7, no. 4: e34397. https://doi.org/10.1371/journal.pone.0034397.

Lonn, E., E. Koskela, T. Mappes, M. Mokkonen, A. M. Sims, and P. C. Watts. 2017. "Balancing Selection Maintains Polymorphisms at Neurogenetic Loci in Field Experiments." *Proceedings of the National Academy of Sciences of the United States of America* 114, no. 14: 3690–3695. https://doi.org/10.1073/pnas.1621228114.

Lotterhos, K. E., and M. C. Whitlock. 2015. "The Relative Power of Genome Scans to Detect Local Adaptation Depends on Sampling Design and Statistical Method." *Molecular Ecology* 24, no. 5: 1031–1046. https://doi.org/10.1111/mec.13100.

Luckenbach, J. A., R. J. Borski, H. V. Daniels, and J. Godwin. 2009. "Sex Determination in Flatfishes: Mechanisms and Environmental Influences." *Seminars in Cell & Developmental Biology* 20, no. 3: 256–263. https://doi.org/10.1016/j.semcdb.2008.12.002.

Mank, J. E. 2017. "Population Genetics of Sexual Conflict in the Genomic Era." *Nature Reviews Genetics* 18, no. 12: 721–730. https://doi.org/10.1038/nrg.2017.83.

Marine Stewardship Council. 2020. "Public Certification Report: Namibia Hake Trawl and Longline Fishery." Prepared on behalf of the Ministry of Marine Resources (MFMR) and the Namibian Hake Association (NHA) by Control Union UK Ltd. Authors: Jones, H., J. Gascoigne, R. Cook, D. Japp, and K. Collinson.

Marine Stewardship Council. 2023. "Marine Stewardship Council (MSC) 2nd Surveillance Audit Report Namibia Hake Trawl and Longline Fishery." https://fisheries.msc.org/en/fisheries/namibia-hake-trawl-and-longline-fishery/@@assessments.

Martínez, P., L. Casas, N. Petit, et al. 2024. "Screening a New European Hake (*Merluccius merluccius*) Chromosome-Level Genome Assembly Suggests an XX/XY Sex Determining System Driven by the *SRY-Box* Transcription Factor 3 (sox3)." *G3: Genes, Genomes, Genetics* 15, no. 8: jkaf127. https://doi.org/10.22541/au.173381838.85727190/v1.

Martínez, P., A. M. Viñas, L. Sánchez, N. Díaz, L. Ribas, and F. Piferrer. 2014. "Genetic Architecture of Sex Determination in Fish: Applications to Sex Ratio Control in Aquaculture." *Frontiers in Genetics* 5: 340. https://doi.org/10.3389/fgene.2014.00340.

McGillycuddy, M., D. I. Warton, G. Popovic, and B. M. Bolker. 2025. "Parsimoniously Fitting Large Multivariate Random Effects in *glmmTMB*." *Journal of Statistical Software* 112, no. 1: 1–19. https://doi.org/10.18637/jss.v112.i01.

Mendoza-Portillo, V., F. J. García-De León, and S. von der Heyden. 2023. "Responses of Population Structure and Genomic Diversity to Climate Change and Fishing Pressure in a Pelagic Fish." *Global Change Biology* 29, no. 14: 4107–4125. https://doi.org/10.1111/gcb.16732.

Moore, E. C., P. J. Ciccotto, E. N. Peterson, M. S. Lamm, R. C. Albertson, and R. B. Roberts. 2022. "Polygenic Sex Determination Produces Modular Sex Polymorphism in an African Cichlid Fish." *Proceedings of the National Academy of Sciences of the United States of America* 119, no. 14: e2118574119. https://doi.org/10.1073/pnas.2118574119.

Nakamoto, M., S. Muramatsu, S. Yoshida, M. Matsuda, Y. Nagahama, and N. Shibata. 2009. "Gonadal Sex Differentiation and Expression of *Sox9a2*, *Dmrt1*, and *Foxl2* in *Oryzias luzonensis*." *Genesis* 47, no. 5: 289–299. https://doi.org/10.1002/dvg.20498.

Narasimhan, V., P. Danecek, A. Scally, Y. Xue, C. Tyler-Smith, and R. Durbin. 2016. "BCFtools/RoH: A Hidden Markov Model Approach for Detecting Autozygosity From Next-Generation Sequencing Data." *Bioinformatics (Oxford, England)* 32, no. 11: 1749–1751. https://doi.org/10.1093/bioinformatics/btw044.

Narum, S. R. 2006. "Beyond Bonferroni: Less Conservative Analyses for Conservation Genetics." *Conservation Genetics* 7, no. 5: 783–787. https://doi.org/10.1007/s10592-005-9056-y.

Niella, Y., P. Butcher, B. Holmes, A. Barnett, and R. Harcourt. 2022. "Forecasting Intraspecific Changes in Distribution of a Wide-Ranging Marine Predator Under Climate Change." *Oecologia* 198, no. 1: 111–124. https://doi.org/10.1007/s00442-021-05075-7.

Nielsen, E. S., S. Walkes, J. L. Sones, et al. 2024. "Pushed Waves, Trailing Edges, and Extreme Events: Eco-Evolutionary Dynamics of a Geographic Range Shift in the Owl Limpet, *Lottia gigantea*." *Global Change Biology* 30, no. 7: e17414. https://doi.org/10.1111/gcb.17414.

Ogle, D. H., J. C. Doll, A. P. Wheeler, and A. Dinno. 2025. "*FSA*: Simple Fisheries Stock Assessment Methods (Version 0.9.6) [R Package]." CRAN. https://CRAN.R-project.org/package=FSA.

Oksanen, J., G. Simpson, F. Blanchet, et al. 2025. "vegan: Community Ecology Package." R Package Version 2.7-1. https://doi.org/10.32614/CRAN.package.vegan, https://CRAN.R-project.org/package=vegan.

Okuda, N., K. Watanabe, K. Fukumori, S. Nakano, and T. Nakazawa. 2014. "A Dynamic Resilience Perspective Toward Integrated Ecosystem Management: Biodiversity, Landscape, and Climate." In *Biodiversity in Aquatic Systems and Environments: Lake Biwa*, edited by N. Okuda, K. Watanabe, K. Fukumori, S. Nakano, and T. Nakazawa, 69–91. Springer Japan. https://doi.org/10.1007/978-4-431-54150-9_4.

Panfili, M., S. Guicciardi O Guizzardi, E. Frapiccini, et al. 2024. "Influence of Contaminants Mercury and PAHs on Somatic Indexes of the European Hake (*Merluccius merluccius*, L. 1758)." *Animals* 14, no. 20: 2938. https://doi.org/10.3390/ani14202938.

Pearse, D. E., N. J. Barson, T. Nome, et al. 2019. "Sex-Dependent Dominance Maintains Migration Supergene in Rainbow Trout." *Nature Ecology & Evolution* 3, no. 12: 1731–1742. https://doi.org/10.1038/s41559-019-1044-6.

Philips, A. E. 2014. "Comparison of Some Biological Aspects Between the Two Sexes of the European Hake *Merluccius merluccius* From the Egyptian Mediterranean Waters." *Egyptian Journal of Aquatic Research* 40, no. 3: 309–315. https://doi.org/10.1016/j.ejar.2014.09.003.

Phillips, N. M., F. Devloo-Delva, C. McCall, and T. S. Daly-Engel. 2021. "Reviewing the Genetic Evidence for Sex-Biased Dispersal in Elasmobranchs." *Reviews in Fish Biology and Fisheries* 31, no. 4: 821–841. https://doi.org/10.1007/s11160-021-09673-9.

Pilastro, A., S. Benetton, and A. Bisazza. 2003. "Female Aggregation and Male Competition Reduce Costs of Sexual Harassment in the Mosquitofish *Gambusia holbrooki*." *Animal Behaviour* 65, no. 6: 1161–1167. https://doi.org/10.1006/anbe.2003.2118.

Pillans, R. D., W. Rochester, R. C. Babcock, D. P. Thomson, M. D. E. Haywood, and M. A. Vanderklift. 2021. "Long-Term Acoustic Monitoring Reveals Site Fidelity, Reproductive Migrations, and Sex Specific Differences in Habitat Use and Migratory Timing in a Large Coastal Shark (*Negaprion acutidens*)." *Frontiers in Marine Science* 8: 616633. https://doi.org/10.3389/fmars.2021.616633.

Pinsky, M. L., and D. Byler. 2015. "Fishing, Fast Growth and Climate Variability Increase the Risk of Collapse." *Proceedings of the Royal Society B: Biological Sciences* 282, no. 1813: 20151053. https://doi.org/10.1098/rspb.2015.1053.

Pinsky, M. L., A. M. Eikeset, C. Helmerson, et al. 2021. "Genomic Stability Through Time Despite Decades of Exploitation in Cod on Both Sides of the Atlantic." *Proceedings of the National Academy of Sciences of the United States of America* 118, no. 15: e2025453118. https://doi.org/10.1073/pnas.2025453118.

Pinsky, M. L., and S. R. Palumbi. 2014. "Meta-Analysis Reveals Lower Genetic Diversity in Overfished Populations." *Molecular Ecology* 23, no. 1: 29–39. https://doi.org/10.1111/mec.12509.

Pinsky, M. L., G. Reygondeau, R. Caddell, J. Palacios-Abrantes, J. Spijkers, and W. W. L. Cheung. 2018. "Preparing Ocean Governance for Species on the Move." *Science* 360, no. 6394: 1189–1191. https://doi.org/10.1126/science.aat2360.

Pinsky, M. L., R. L. Selden, and Z. J. Kitchel. 2020. "Climate-Driven Shifts in Marine Species Ranges: Scaling From Organisms to Communities." *Annual Review of Marine Science* 12, no. 1: 153–179. https://doi.org/10.1146/annurev-marine-010419-010916.

Privé, F., K. Luu, B. J. Vilhjálmsson, and M. G. B. Blum. 2020. "Performing Highly Efficient Genome Scans for Local Adaptation With R Package *Pcadapt* Version 4." *Molecular Biology and Evolution* 37, no. 7: 2153–2154. https://doi.org/10.1093/molbev/msaa053.

Pujolar, J. M., C. E. C. Gardiner, S. von der Heyden, et al. 2025. "Resolving the Population Structure and Demographic History of the European Anchovy in the Northeast Atlantic: Tracking Historical and Contemporary Environmental Changes." *Molecular Ecology* 34, no. 14: e17829. https://doi.org/10.1111/mec.17829.

Purcell, S., B. Neale, K. Todd-Brown, et al. 2007. "PLINK: A Tool Set for Whole-Genome Association and Population-Based Linkage Analyses." *American Journal of Human Genetics* 81, no. 3: 559–575. https://doi.org/10.1086/519795.

R Core Team. 2023. "*R*: A Language and Environment for Statistical Computing." R Foundation for Statistical Computing, Vienna, Austria. https://www.R-project.org/.

Ramos, J. E., G. T. Pecl, N. A. Moltschaniwskyj, J. M. Semmens, C. A. Souza, and J. M. Strugnell. 2018. "Population Genetic Signatures of a Climate Change Driven Marine Range Extension." *Scientific Reports* 8, no. 1: 9558. https://doi.org/10.1038/s41598-018-27351-y.

Reichard, M., M. Polačik, R. Blažek, and M. Vrtílek. 2014. "Female Bias in the Adult Sex Ratio of African Annual Fishes: Interspecific Differences, Seasonal Trends and Environmental Predictors." *Evolutionary Ecology* 28, no. 6: 1105–1120. https://doi.org/10.1007/s10682-014-9732-9.

Reygondeau, G., L. Guidi, G. Beaugrand, et al. 2017. "Global Biogeochemical Provinces of the Mesopelagic Zone." *Journal of Biogeography* 45, no. 2: 500–514. https://doi.org/10.1111/jbi.13149.

Roberts, N. B., S. A. Juntti, K. P. Coyle, et al. 2016. "Polygenic Sex Determination in the Cichlid Fish *Astatotilapia burtoni*." *BMC Genomics* 17, no. 1: 835. https://doi.org/10.1186/s12864-016-3177-1.

Robinson, C., D. K. Steinberg, T. R. Anderson, et al. 2010. "Mesopelagic Zone Ecology and Biogeochemistry–a Synthesis." *Deep Sea Research, Part II: Topical Studies in Oceanography* 57, no. 16: 1504–1518. https://doi.org/10.1016/j.dsr2.2010.02.018.

Rouault, M., B. Pohl, and P. Penven. 2010. "Coastal Oceanic Climate Change and Variability From 1982 to 2009 Around South Africa." *African Journal of Marine Science* 32, no. 2: 237–246. https://doi.org/10.2989/1814232X.2010.501563.

Schulze, M. J., S. von der Heyden, D. Japp, et al. 2020. "Supporting Fisheries Management With Genomic Tools: A Case Study of Kingklip (*Genypterus capensis*) Off Southern Africa." *Frontiers in Marine Science* 7: 557146. https://doi.org/10.3389/fmars.2020.557146.

Shafer, A. B. A., and M. Kardos. 2025. "Runs of Homozygosity and Inferences in Wild Populations." *Molecular Ecology* 34, no. 3: e17641. https://doi.org/10.1111/mec.17641.

Shillington, F. A., C. J. C. Reason, C. D. Rae, P. Florenchie, and P. Penven. 2006. "Large Scale Physical Variability of the Benguela Current Large Marine Ecosystem (BCLME)." In *Large Marine Ecosystems*, vol. 14, 49–70. Elsevier.

Slotte, A., A. Salthaug, S. Vatnehol, et al. 2025. "Herring Spawned Poleward Following Fishery-Induced Collective Memory Loss." *Nature* 642: 1–8. https://doi.org/10.1038/s41586-025-08983-3.

Somjee, U., A. Shankar, and J. J. Falk. 2022. "Can Sex-Specific Metabolic Rates Provide Insight Into Patterns of Metabolic Scaling?" *Integrative and Comparative Biology* 62, no. 5: 1460–1470. https://doi.org/10.1093/icb/icac135.

St. John, M. A., A. Borja, G. Chust, et al. 2016. "A Dark Hole in Our Understanding of Marine Ecosystems and Their Services: Perspectives From the Mesopelagic Community." *Frontiers in Marine Science* 3: 31. https://doi.org/10.3389/fmars.2016.00031.

Storey, J. D., A. J. Bass, A. Dabney, and D. Robinson. 2023. "*qvalue*: Q-Value Estimation for False Discovery Rate Control." https://doi.org/10.18129/B9.bioc.qvalue.

Strømme, T., M. R. Lipinski, and P. Kainge. 2016. "Life Cycle of Hake and Likely Management Implications." *Reviews in Fish Biology and Fisheries* 26, no. 2: 235–248. https://doi.org/10.1007/s11160-015-9415-9.

Struch, R. E., E. L. Pulster, A. D. Schreier, and S. A. Murawski. 2019. "Hepatobiliary Analyses Suggest Chronic PAH Exposure in Hakes (*Urophycis* spp.) Following the Deepwater Horizon Oil Spill." *Environmental Toxicology and Chemistry* 38, no. 12: 2740–2749. https://doi.org/10.1002/etc.4596.

Sumaila, U. R., C. De Fontaubert, and M. L. D. Palomares. 2023. "How Overfishing Handicaps Resilience of Marine Resources Under Climate Change." *Frontiers in Marine Science* 10: 1250449. https://doi.org/10.3389/fmars.2023.1250449.

Teske, P., S. von der Heyden, C. McQuaid, and N. Barker. 2011. "A Review of Marine Phylogeography in Southern Africa." *South African Journal of Science* 107, no. 5: 1–11. https://doi.org/10.10520/EJC9714.

Teske, P. R., A. Emami-Khoyi, T. R. Golla, et al. 2021. "The Sardine Run in Southeastern Africa Is a Mass Migration Into an Ecological Trap." *Science Advances* 7, no. 38: eabf4514. https://doi.org/10.1126/sciadv.abf4514.

Tobler, M., I. Schlupp, and M. Plath. 2011. "Costly Interactions Between the Sexes: Combined Effects of Male Sexual Harassment and Female Choice?" *Behavioral Ecology* 22, no. 4: 723–729. https://doi.org/10.1093/beheco/arr044.

Vandeputte, M., M. Dupont-Nivet, H. Chavanne, and B. Chatain. 2007. "A Polygenic Hypothesis for Sex Determination in the European Sea Bass *Dicentrarchus labrax*." *Genetics* 176, no. 2: 1049–1057. https://doi.org/10.1534/genetics.107.072140.

Voldoire, E., F. Brunet, M. Naville, J.-N. Volff, and D. Galiana. 2017. "Expansion by Whole Genome Duplication and Evolution of the *Sox* Gene Family in Teleost Fish." *PLoS One* 12, no. 7: e0180936. https://doi.org/10.1371/journal.pone.0180936.

von der Heyden, S., M. Beger, R. J. Toonen, et al. 2014. "The Application of Genetics to Marine Management and Conservation: Examples From the Indo-Pacific." *Bulletin of Marine Science* 90: 123–158. https://doi.org/10.5343/bms.2012.1079.

von der Heyden, S., M. R. Lipinski, and C. A. Matthee. 2007a. "Mitochondrial DNA Analyses of the Cape Hakes Reveal an Expanding, Panmictic Population for *Merluccius Capensis* and Population Structuring for Mature Fish in *Merluccius paradoxus*." *Molecular Phylogenetics and Evolution* 42, no. 2: 517–527. https://doi.org/10.1016/j.ympev.2006.08.004.

von der Heyden, S., M. R. Lipinski, and C. A. Matthee. 2007b. "Species-Specific Genetic Markers for Identification of Early Life-History Stages of Cape Hakes, *Merluccius Capensis* and *Merluccius Paradoxus* in the Southern Benguela Current." *Journal of Fish Biology* 70: 262–268. https://doi.org/10.1111/j.1095-8649.2007.01409.x.

Wang, J., Z. Y. Cheng, and Y. W. Dong. 2022. "Demographic, Physiological and Genetic Factors Linked to the Poleward Range Expansion of the Snail *Nerita yoldii* Along the Shoreline of China." *Molecular Ecology* 31, no. 17: 4510–4526. https://doi.org/10.1111/mec.16610.

Waples, R. S., and A. Audzijonyte. 2016. "Fishery-Induced Evolution Provides Insights Into Adaptive Responses of Marine Species to Climate

Change." *Frontiers in Ecology and the Environment* 14, no. 4: 217–224. https://doi.org/10.1002/fee.1264.

Wiberg, R. A. W., P. Veltsos, R. R. Snook, and M. G. Ritchie. 2021. "Experimental Evolution Supports Signatures of Sexual Selection in Genomic Divergence." *Evolution Letters* 5, no. 3: 214–229. https://doi.org/10.1002/evl3.220.

Wickham, H. 2007. "Reshaping Data With the *Reshape* Package." *Journal of Statistical Software* 21, no. 12: 1–20. https://doi.org/10.18637/jss.v021.i12.

Wickham, H. 2016. *ggplot2: Elegant Graphics for Data Analysis*. Springer-Verlag. https://doi.org/10.1007/978-3-319-24277-4.

Wilhelm, M. R., B. A. Black, T. Lamont, S. C. Paulus, C. Bartholomae, and D. C. Louw. 2020. "Northern Benguela *Merluccius paradoxus* Annual Growth From Otolith Chronologies Used for Age Verification and as Indicators of Fisheries-Induced and Environmental Changes." *Frontiers in Marine Science* 7: 315. https://doi.org/10.3389/fmars.2020.00315.

Wilhelm, M. R., C. H. Kirchner, J. P. Roux, et al. 2015. "Biology and Fisheries of the Shallow-Water Hake (*Merluccius capensis*) and the Deep-Water Hake (*M. paradoxus*) in Namibia. Chapter 3." In *Hakes: Biology and Exploitation*, edited by H. Arancibia, 70–100. John Wiley & Sons, Ltd. https://doi.org/10.1002/9781118568262.ch3.

Wright, A. E., M. Fumagalli, C. R. Cooney, et al. 2018. "Male-Biased Gene Expression Resolves Sexual Conflict Through the Evolution of Sex-Specific Genetic Architecture." *Evolution Letters* 2, no. 2: 52–61. https://doi.org/10.1002/evl3.39.

Wu, G.-C., P.-C. Chiu, Y.-S. Lyu, and C.-F. Chang. 2010. "The Expression of *Amh* and *amhr2* Is Associated With the Development of Gonadal Tissue and Sex Change in the Protandrous Black Porgy, *Acanthopagrus Schlegeli*." *Biology of Reproduction* 83, no. 3: 443–453. https://doi.org/10.1095/biolreprod.110.084681.

Yokoi, H., T. Kobayashi, M. Tanaka, et al. 2002. "*sox9* in a Teleost Fish, Medaka (*Oryzias latipes*): Evidence for Diversified Function of *Sox9* in Gonad Differentiation." *Molecular Reproduction and Development* 63, no. 1: 5–16. https://doi.org/10.1002/mrd.10169.

Zeileis, A., and G. Grothendieck. 2005. "*Zoo*: S3 Infrastructure for Regular and Irregular Time Series." *Journal of Statistical Software* 14, no. 6: 1–27. https://doi.org/10.18637/jss.v014.i06.

Zhang, C., S.-S. Dong, J.-Y. Xu, W.-M. He, and T.-L. Yang. 2019. "*PopLDdecay*: A Fast and Effective Tool for Linkage Disequilibrium Decay Analysis Based on Variant Call Format Files." *Bioinformatics* 35, no. 10: 1786–1788. https://doi.org/10.1093/bioinformatics/bty875.

Zhao, K., S. D. Gaines, J. García Molinos, M. Zhang, and J. Xu. 2022. "Climate Change and Fishing Are Pulling the Functional Diversity of the World's Largest Marine Fisheries to Opposite Extremes." *Global Ecology and Biogeography* 31, no. 8: 1616–1629. https://doi.org/10.1111/geb.13534.

Supporting Information

Additional supporting information can be found online in the Supporting Information section. **Figure S1:** Spatial distribution of *Merluccius paradoxus* along the South African coastline based on fishery-independent demersal research surveys conducted on (a) the West Coast in February 2022 and the South Coast in April 2021 by the Fisheries branch of the Department of Forestry, Fisheries, and the Environment, South Africa. The proportion of males are shown in dark purple, and females in light purple. Black circles represent sampling stations where *M. paradoxus* was absent. Circle size represents the log-transformed total catch (kg), while line weight and style denote different depth intervals (isobaths). **Figure S2:** Distance-based redundancy analysis (dbRDA) of 2,347,710 SNP data from 37 Merluccius paradoxus samples along the southern African coastline. Individuals are coloured by region, with sex indicated by point shape (circles represent females, and triangles represent males). Arrows represent predictor variables included in the model, with arrow length indicating the strength of their contribution to genetic differentiation. Significance levels for predictor variables are denoted as follows: $p < 0.001$ (***), $p < 0.01$ (**), $p < 0.05$ (*) and $p > 0.05$ (blank). **Figure S3:** Principal component analysis (PCAs) of 2,347,710 SNP data for all 37 M. paradoxus samples from the southern African coastline. Each plot displays the first and second principal components. Individuals are coloured by sequencing batch (a) and sequencing coverage (b) respectively with sex denoted by point shape: circles represent females, and triangles represent males. A 95% confidence interval ellipse is drawn around male and female clusters to indicate group dispersion. **Figure S4:** Multidimensional scaling (MDS) plot based on identity-by-missingness (IBM) analysis using the filtered SNP dataset (2,347,710 SNPs) for 37 *M. paradoxus* samples. Individuals are coloured by region, with sex indicated by point shape (circles represent females, and triangles represent males). **Figure S5:** Principal component analyses (PCAs) of (a) outlier (53,522 SNPs) and (b) neutral (2,294,188 SNPs) datasets for all 37 *Merluccius paradoxus* samples from the southern African coastline. Each plot displays the first and second principal components. Individuals are coloured by region, with sex denoted by point shape: circles represent females, and triangles represent males. **Figure S6:** Genome-wide pairwise Weir and Cockerham F_{ST} estimates between West Edge ($n = 10$) and East Edge ($n = 8$) female *Merluccius paradoxus* individuals, based on 2,347,710 SNPs. The grey dashed line indicates the 99th percentile threshold for F_{ST} values observed in male-female comparisons across the genome. **Figure S7:** BayeScan results for 58, 100 SNPs found on Chromosome 2 in *Merluccius paradoxus*. The plot shows the relationship between F_{ST} and log-transformed q-values where each point represents a SNP. SNPs are coloured according to the type of selection they are under namely, balancing selection (white; $q < 0.05$, $a < 0$), diversifying selection (red; $q < 0.05$, $a > 0$) and neutral SNPs (orange; $q > 0.05$). **Figure S8:** Principal component analysis (PCAs) of 1,173,439 SNPs that were retained after filtering for linkage disequilibrium ($r^2 > 0.2$) for all 37 *Merluccius paradoxus* samples. Each plot displays the first and second principal components. Individuals are coloured by region, with sex denoted by point shape: circles represent females, and triangles represent males. A 95% confidence interval ellipse is drawn around male and female clusters to indicate group dispersion. **Figure S9:** Genomic inbreeding coefficient (F_{ROH}) for males and females across sampling locations, based on 2,347,710 SNPs. Violin plots show the distribution of F_{ROH} within each sex-population group with embedded boxplots representing the data spread. The bold line within each box indicates the median, while the upper and lower box edges correspond to the interquartile range. **Figure S10:** Genome-wide nucleotide diversity (; a) and runs of homozygosity (ROH) density (b) for the individuals collected from the West Edge (orange; originally Namibia), Core (turquoise; originally West and South Coast), and East Edge (purple; originally Eastern Cape) of the *Merluccius paradoxus* distribution, based on 2,347,710 SNPs. Chromosomes are separated by grey dashed lines on the x-axis. The right of each panel shows a zoomed-in view of chromosomes of interest, highlighting sex-specific genomic patterns. Nucleotide diversity ($\boldsymbol{\pi}$; a) was calculated in 50kb windows, and ROH density (b) was calculated in 2Mb bins along the genome. **Figure S11:** Genome-wide Tajima's D (a) and observed heterozygosity (H_o; b) for *Merluccius paradoxus*, based on 2,347,710 SNPs for each sampling location. Chromosomes are separated by grey dashed lines on the x-axis, with regions of interest highlighted by grey dashed boxes. Panel A shows Tajima's D in 150kb windows for the West Edge (orange; originally Namibia), Core (turquoise; originally West and South Coast) and East Edge (purple; originally Eastern Cape) of the distribution. Right panels show observed heterozygosity (per SNP, 50 kb windows) for windows for the West Edge (orange; originally Namibia), Core (turquoise; originally West and South Coast) and East Edge (purple; originally Eastern Cape) of the distribution. **Figure S12:** The number of runs of homozygosity (ROH) within three length categories (short, medium and long) across sexes and sampling locations, based on 2,347,710 SNPs. Box plots represent the distribution of ROH counts within each category: short ROH (< 20 kb), medium ROH (20–100 kb) and long (> 100 kb). The bold line within each box indicates the median, while the upper and lower box edges correspond to the

interquartile range. **Figure S13:** Linkage disequilibrium (LD) decay across the genome (a) and on Chromosome 2 for all individuals (b), for males (c) and for females (d) in *Merluccius paradoxus*. LD was measured as mean pairwise r^2 and plotted as a function of distance (bp) between SNPs within a 500Kb window. **Figure S14:** Linkage disequilibrium (LD) heatmaps showing mean pairwise r^2 values between SNPs on Chromosome 2 in *Merluccius paradoxus*. Heatmaps are shown for (a) all individuals, (b) males and (c) and females. Colour indicates the strength of LD, with green representing higher r^2 values and purple representing lower r^2 values. **Figure S15:** Sankey plot summarizing significantly enriched GO terms from the gene ontology (GO) enrichment analysis for genomic regions with high-F_{ST} between males and females on Chromosomes 1 and 2. The pot displays GO terms and their classification into primary and secondary functional groups. **Table S1:** Summary of *Merluccius paradoxus* samples sequenced for this study. The table includes the sample sites, the number of samples per region (*N*), the number of samples collected per location (*n*), geographic coordinates (decimal degrees), depth (meters) and the month and year of sample collection. **Table S2:** Summary of distance-based redundancy analysis (dbRDA) results for the reduced model examining the effects of depth, length, longitude, maturity and sex on genetic variation in *Merluccius paradoxus*. Genetic variation is based on 2,347,710 SNPs from 37 individuals sampled along the southern African coastline. Significance levels for predictor variables are denoted as follows: $p < 0.001$ (***), $p < 0.01$ (**), $p < 0.05$ (*) and $p > 0.05$ (blank). **Table S3:** Global weighted pairwise Weir and Cockerham F_{ST} estimates for *Merluccius paradoxus* based on 2,347,710 SNPs, calculated between four sampling locations along the southern African coastline. Significance levels are indicated as follows: *$p < 0.05$; **$p < 0.01$; ***$p < 0.001$. **Table S4:** Average measures of genomic diversity for each location and sex, based on 2,347,710 SNPs: *n*–number of individuals; $\boldsymbol{\pi}$–nucleotide diversity (per site); D–Tajima's D (50 kb windows); H_o–observed heterozygosity (per site); H_e–expected heterozygosity (per site); FIS–inbreeding coefficient (per individual); F_{ROH}–genomic inbreeding coefficient. Standard error values are reported in brackets next to each mean.